Copyright Warning & Restrictions

The copyright law of the United States (Title 17, United States Code) governs the making of photocopies or other reproductions of copyrighted material.

Under certain conditions specified in the law, libraries and archives are authorized to furnish a photocopy or other reproduction. One of these specified conditions is that the photocopy or reproduction is not to be "used for any purpose other than private study, scholarship, or research." If a, user makes a request for, or later uses, a photocopy or reproduction for purposes in excess of "fair use" that user may be liable for copyright infringement,

This institution reserves the right to refuse to accept a copying order if, in its judgment, fulfillment of the order would involve violation of copyright law.

Please Note: The author retains the copyright while the New Jersey Institute of Technology reserves the right to distribute this thesis or dissertation

Printing note: If you do not wish to print this page, then select "Pages from: first page # to: last page #" on the print dialog screen

ABSTRACT

A Mathematical Model for the Prediction of Depth of Cut in the Course of AWJ Machining

by Naijian Ma

The objective of this study is to develop a practical mathematical model for prediction of the depth of cut in the course of Abrasive Water Jet (AWJ) machining. Semi-empirical method which is an integration of theoretical derivation and statistical analysis is used for process description. A theoretical model was constructed based on kinetic energy conservation equation, physical relationship among operating parameters, abrasive size, material properties and cutting results. Then, correlation between the depth of cut and operational parameters was analyzed in order to improve the theoretical model. Finally, a regression equation representing 1000 samples was constructed.

Three statistical criteria were considered synthetically to determine the final form of the regression equation. These criteria include multiple correlation coefficient R^2, the plot of a standard residual g_i, and the number of $g_i > \pm 2$.

The multiple correlation coefficients for evaluation of the accuracy of the constructed equation range from 0.95 to 0.99. Prediction error in 92% of cases did not exceed ± 2 mm for samples having thickness up to 30 mm. The constructed equation was also used for process examination. It was evaluated, for example, that water contribution to the material removal is roughly 10 times less than particles contribution.

A MATHEMATICAL MODEL FOR THE PREDICTION OF DEPTH OF CUT IN THE COURSE OF AWJ MACHINING

by
Naijian Ma

A Thesis
Submitted to the Faculty of
New Jersey Institute of Technology
in Partial Fulfillment of the Requirements for the Degree of
Master of Science in Mechanical Engineering

Department of Mechanical and Industrial Engineering

May 1993

APPROVAL PAGE

A Mathematical Model for the Prediction of Depth of Cut in the Course of AWJ Machining

Naijian Ma

Dr. Ernest S. Geskin, Thesis Advisor (date)
Professor of Mechanical Engineering, NJIT

Dr. Rong-Yaw Chen, Committee Member (date)
Professor of Mechanical Engineering, NJIT

Dr. Zhiming Ji, Committee Member (date)
Assistant Professor of Mechanical Engineering, NJIT

BIOGRAPHICAL SKETCH

Author : Naijian Ma

Degree : Master of Science in Mechanical Engineering

Date : May 1993

Undergraduate and Graduate Education:

- Master of Science in Mechanical Engineering
  New Jersey Institute of Technology, Newark, New Jersey
  1993

- Bachelor of Science in Mechanical Engineering
  China Textile University, Shanghai, P. R. China
  1983

Major : Mechanical Engineering

This thesis is dedicated to a good friend of mine, Mr. Baichuan Wang.

ACKNOWLEDGMENT

The author wishes to express his sincere gratitude to his advisor, Professor Ernest S. Geskin, for his guidance, patience and moral support throughout this study.

Special thanks to Dr. Chen and Dr. Ji for their helpful suggestions and valuable comments. The author appreciates the timely help and suggestions from all the Waterjet Laboratory members.

Finally, a grateful thank you to the author's wife, Hong Zhu, and his parents for their firm support and encouragement.

TABLE OF CONTENTS

Chapter **Page**

LIST OF TABLES

LIST OF FIGURES

Figure **Page**

Figure **Page**

NOMENCLATURE

A	The order of M_a determined by regression analysis
B	The order of D_t determined by regression analysis
Ca	Coefficient for the cutting efficiency of Abrasive
C_o, C_1, C_2, C_3	Regression coefficient determined by regression analysis
D_o	Diameter of sapphire orifice (mm)
D_t	Diameter of carbide tube (mm)
Ea	Abrasive kinetic energy at the exit of the tube($N \cdot m / min$)
Ew	Water kinetic energy at the exit of the tube($N \cdot m / min$)
gi	Standard Residual
H_w	Fitted depth of cut caused by water action (mm)
H_a	Fitted depth of cut caused by abrasive action (mm)
H_I	Fitted depth of cut caused by the interaction between water and abrasive(mm)
H	Total observed depth of cut by AWJ (mm)
$\hat{H}$	Total fitted depth of cut (mm)
Ka	Coefficient of abrasive velocity at the exit of the tube
Kw	Coefficient of water velocity at the exit of the tube
M_a	Mass flow rate of abrasive (g/min)
M_w	Mass flow rate of water (g/min)
P_w	Percentage of water action on the depth of cut (%)
P_a	Percentage of abrasive action on the depth of cut (%)
P_i	Initial water pressure (MPa)
P_o	Operating water pressure (MPa)
R^2	Correlation coefficient
S_a	Size of abrasive (mesh)

S_d	Standoff distance (mm)
$S^2_{y/x}$	Conditional sample variance of y
U	Traverse speed of the nozzle (cm/min)
V_{sw}	Water velocity at the exit of sapphire nozzle (m/min)
V_{cw}	Water velocity at the exit of carbide nozzle (m/min)
V_a	Abrasive particle velocity at the exit of carbide nozzle (m/min)
Vm	Mixed slurry velocity at the exit of the tube (m/min)
W	Work done by the cutting force of AWJ($N \cdot m / min$)
W_t	Top kerf width (mm)
ρ_w	Water density (kg/cm3)
σ	Flow strength of the material (MPa)

CHAPTER 1
INTRODUCTION

Abrasive Waterjet (AWJ) machining is as a new manufacture technology used for cutting, milling and cleaning a variety of metal and non-metal materials[1]. The abrasive waterjet is formed by entraining abrasive particles by high-velocity waterjet (WJ) in the mixing chamber of a nozzle body. WJ creates the vacuum in this chamber and abrasive particles are sucked into the chamber as shown in Fig 1. Water and abrasive particles are then introduced into a focusing tube where the turbulent pulsation assures mixing of two phases and forming of abrasive waterjet. Here, part of the momentum of the waterjet is transferred to the abrasive particles and particles velocity abruptly increases. As a result of the momentum transfer between the water and particles, a high-velocity slurry of abrasive is generated. This slurry can be used for machining almost all ductile and brittle materials including those which can not be cut by the conventional cutting techniques.

One of important elements of AWJ technology is evaluation of the relationship between depth of cut and process parameters [2-9]. There are three feasible approaches for the mathematical modeling of this relationship. The first is construction of an empirical model based on the statistical analysis of experimental data. The second approach involves theoretical analysis of cutting. The final one is the combination of empirical and theoretical methods. This semi-empirical method is employed in our study. A developed model includes the following variables:

- waterjet pressure (Po)
- waterjet orifice diameter (D_o)
- focusing tube diameter (D_t)
- traverse speed of nozzle (u)
- standoff distance (S_d = 2.5mm in this study)
- abrasive mass flow rate (m_a)

- size of particle (S_a)

- abrasive material (garnet sand was used in this study)

- material property (flow stress σ was used in this work)

The objectives of this study were to

(1) establish a new mathematical model for predicting the depth of cut.

(2) investigate comparative effects of water and particle actions on the depth of cut.

(3) evaluate effects of various process parameters on the depth of cut.

(4) study the distribution of water and abrasive particles velocities at the exit of carbide tube.

The previous studies of the AWJ working mechanism are discussed in chapter 2. Statistical methods used in this study are discussed in chapter 3. The experimental apparatus and methods are presented in Chapter 4 and a new model for prediction of depth of cut by AWJ is constructed and presented in chapter 5. The prediction results and some inferences on AWJ cutting are discussed in chapter 6. Conclusions and recommendations are given in chapter 7.

CHAPTER 2

PREVIOUS RESEARCH SURVEY

Abrasive waterjet machining is a new manufacturing technology which combines the principles of waterjet and abrasive jet machining and creates a unique process that has applied to cutting, drilling milling and cleaning by means of the erosion action of a slurry jet.

2.1 The Study of the Basic Theory of AWJ Machining

The most studies reduced the mechanism of AWJ machining to the workpiece-particle interaction and several theoretical models were constructed on this basis [10-19]. This approach is based on the pioneering studies of Finnie and Bitter who studied the erosion mechanism and established the equations relating volume removed by AWJ with physical and geometric process characteristics.

Finnie [20] studied an impact of a rigid abrasive grain onto a ductile metal. He derived the equations describing the trajectory of an individual particle of mass M striking a solid surface at an angle α with a velocity V as shown in Fig 2.

It was assumed that the center of the particle translates in x and y directions while the particles is turned at angle ϕ. The particle is considered as the cutting edge of a tool penetrating into a ductile material. The volume removal W can be found by integrating the equations of the particle motion over the period of penetration. The final equations yield:

$$W = \frac{m V^2}{PCK}\left(\mathrm{Sin}(2\alpha) - \frac{6}{K}\mathrm{Sin}^2\alpha\right) \qquad \text{if} \quad \tan\alpha \le \frac{K}{6} \qquad (2.1)$$

$$W = \frac{mV^2}{PCK}\left(\frac{K\cos^2\alpha}{6}\right) \qquad \text{if} \quad \tan\alpha \geq \frac{K}{6} \tag{2.2}$$

Where

W : the volume removed by an abrasive particle

P : horizontal component of the stress on the particle face

C : the ratio L/y_t

K : the ratio of vertical to horizontal force component acting on particle

m : amount of abrasive

V : velocity of a particle

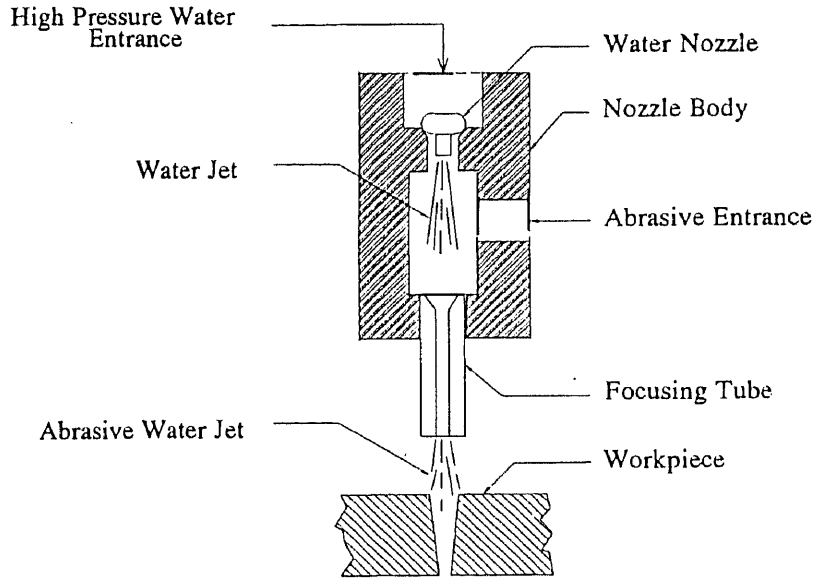

Figure 1 Schematic of Cutting Nozzle Body

The results of the prediction by the above equations were compared with test results from a specially designed "sandblast" type tester in which the velocity, direction, and amount of abrasive were carefully controlled. It was found that for ductile materials it

is possible to predict the manner in which material removal varies with the direction and velocity of the eroding particles.

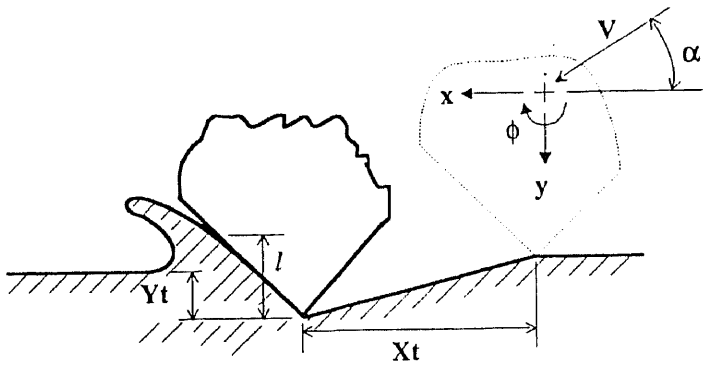

Figure 2 The Ideal Model of a Abrasive Impinging on the Ductile Material

Bitter [21] studied the erosion by solid particles in a different way. He found that the cutting surface of the workpiece exhibits two distinctive regions. The top area of the cutting surface is smoother than the bottom one in which obvious striations exist (Fig 3). According to Bitter the erosion by solid particles is divided into two types. One (the upper region) is called cutting wear which had been analyzed by Finnie, another one (the lower region) is termed deformation wear that corresponds to the erosion at almost normal angle of attack on ductile materials. Bitter derived the equation of deformation wears using the energy balance of collisions at large angles. The resulting equation for deformation and cutting wear derived by Bitter[21] are given below:

$$W_D = \frac{1}{2}\frac{M(V\sin\alpha - V_C)^2}{E_O} \qquad 0 \le \alpha \le 90^\circ \qquad (2.3)$$

$$W=\frac{2MC(V\sin\alpha-V_C)}{\sqrt{V\sin\alpha}}\left[V\cos\alpha-\frac{C(V\sin\alpha-V_C)^2}{\sqrt{V\sin\alpha}}\rho\right] \qquad \alpha \le \alpha_o \qquad (2.4)$$

$$W_C=\frac{\frac{1}{2}M\left[V^2\cos\alpha-K_1(V\sin\alpha-V_C)\right]}{\rho} \qquad \alpha \ge \alpha_o \qquad (2.5)$$

where

W_D, W_C: units volume loss due to deformation wear and cutting wear, respectively

M : total mass of impinging particles

V : particles velocity

α : impact angle

V_C : maximum particle velocity at which the collision is still purely elastic

E_o: the energy needed to removed a unit volume of material from the body by deformation wear(deformation wear factor)

ρ : the energy needed to scratch out a unit volume from a surface (cutting wear factor)

constant : $C=\frac{0.288}{y}\sqrt[4]{d/y}$

constant : $0.82\,y^2\sqrt[4]{y/d}\left(\frac{1-q_1^2}{E_1}+\frac{1-q_2^2}{E_2}\right)^2$

y : elastic load limit

d : density

E : young's modules

q : poisson's ratio

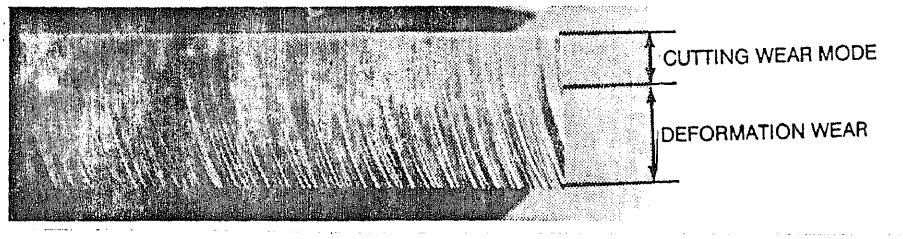

Figure 3 The Striations in the Cutting Surface

It is obvious that Bitter's equations include both elastic and plastic properties of the particles and specimen materials. This is an intricate study. The following assumptions have been made.

(1) The normal component of kinetic energy of the impacted particles is absorbed in the specimen surface and accounts for deformation wear.

(2) For certain hard materials, subjected principally to deformation wear, there is a limiting component of velocity normal to the surface below which no erosion takes place. This limiting value depends on the particle shape.

(3) The kinetic energy component parallel to the surface is associated with cutting wear.

(4) For cutting wear and large angles of attack the particles come to rest of the surface and the total parallel component of kinetic energy contributes to cutting wear. For the small angle of attack, however, the particles may sweep into the surface and finally leave again with a residual amount of parallel kinetic energy.

Neilson and Gilchrish [22] also established a similar simplified model for erosion by a stream of solid particles as follows:

$$W = \underbrace{\frac{\frac{1}{2}MV^2\cos^2\sin(n\alpha)}{\rho}}_{(A)} + \underbrace{\frac{\frac{1}{2}M(V\sin\alpha - K)^2}{E_o}}_{(B)} \qquad \alpha < \frac{\pi}{2n} \tag{2.6}$$

$$W = \underbrace{\frac{\frac{1}{2}M V^2 \cos^2\alpha}{\rho}}_{(C)} + \underbrace{\frac{\frac{1}{2}M(V\sin\alpha - K)^2}{E_o}}_{(B)} \qquad \alpha \rangle \frac{\pi}{2n} \qquad (2.7)$$

where

W : the erosion produced by M pounds of particles at the angle of attack α and particles velocity V

K : the velocity component normal to the surface below which no erosion takes place

Actually, part B accounts for deformation wear and part A and C account for cutting wear at the small and large angles of attack, respectively.

In 1987, Hashish developed an improved model for the erosion by solid particles in a liquid jet. According to Hashish erosion of ductile metals by sharp particle, impact is related to the particle velocity to powers greater than 2, but less than 3 [23,24]. The existing models, however, are not satisfactory in accounting for this dependency. Also, these models do not account for particle size or shape. Hashish expanded Finnie's model including the crater width variation as the depth of the trajectory varies.

The resulting model shows a velocity exponent of 2.5 and includes the particle shape expressed by its sphericity and roundness numbers. This improved model is best suited for shallow angles of impact and is expressed as :

$$\delta v = \frac{7}{\pi}\frac{m}{\rho_p}\left(\frac{V}{C_k}\right)^{2.5} \sin(2\alpha)\sqrt{\sin\alpha} \qquad (2.8)$$

Where

δv : volume removed

m : mass of particle

ρ_p : density of particle

V : particle velocity

α : impact angle

In the equation (2.8), C_k is a characteristic velocity that combines particle and material characteristics :

$$C_k = \sqrt{\frac{3\sigma R_f^{3/5}}{\rho_p}}$$

where

σ : material flow stress

R_f : particles roundness

2.2 The Study of the Models for Predicting Cutting Results

The modeling for predicting the cutting results is an important element in the study of AWJ. Three approaches are possible for constructing the mathematical model of a phenomena in question. The first one is constructing pure empirical model, which has the general form as follows:

$$H = C_o A_1^{x_1} A_2^{x_2} A_3^{x_3} \ldots\ldots A_n^{x_n} \qquad (2.9)$$

where

H : depth of cut

$A_1 \ldots A_n$: relative parameters or combination of the parameters

$X_1 \ldots X_n$: the power corresponding to $A_1 \ldots A_n$

Co: regression coefficient

Several such studies on the empirical model have been reported since 1980's. The example for that is the work[25] which suggested the following regression equation:

$$h/d = K_O[S_r(P/\sigma)(d/S)(V_j t/d)^{0.5}]\alpha \qquad (2.10)$$

where

h : depth of cut

d : nozzle diameter

K_O , α : constants

S_r : stroke ratio

P : jet pressure

S : standoff distance

V_j : jet velocity

t : pulse duration

σ : material tensile strength

The second approach is the construction of a theoretical model for process prediction in which an example is Hashish's equation [26]:

$$h_c = \frac{(V_C/C_K)d_j}{\left(\frac{\pi\rho_p u d_j}{14 m_a}\right)^{2/5} + \frac{V_e}{C_K}} \tag{2.11}$$

$$h_d = \frac{1}{\frac{\pi D_j \sigma u}{2 C_l m_a (V_O - V_e)^2} + \frac{C_f}{D_j}\frac{V_o}{(V_o - V_e)}} \tag{2.12}$$

where

$C_k = \sqrt{\frac{3\sigma R_f^{3/5}}{\rho_p}}$: characteristic velocity

h_c, h_d : depth of cut due to cutting wear and deformation wear mode, respectively

V_o : initial particle velocity

V_e : threshold particle velocity

D_j : jet diameter

ρ_p : density of particle

σ : material flow stress

R_f : particle roundness factor

C_f : coefficient of friction on kerf wall

m_a : abrasive flow rate

C_1 : ratio of m_a in which particles cause material removal

u : jet traverse rate

In Hashish's model the total depth of cut was divided into two distinct zones due to different modes of interaction between impinging abrasive particles and the target material as indicated in Fig 3. The upper zone is due to a cutting wear mode at shallow angles of impact. The lower zone is due to a deformation wear mode at large angles of impact. Hashish applied a number of parameters including operating parameters, geometric parameters and material properties to his theoretical model. As reported, the correlation coefficient for many of the metals is over 0.9. But, this model is only a theoretical derived product because part of the parameters such as R_f, C_f, C_1 are selected arbitrarily although it contains most of relative parameters. It also should be pointed out that this model only considers particle action, while omits the water action.

The third approach, termed semi-empirical method, combines empirical statistical and pure theoretical methods. An example of such approach is Chung's equation [27]

$$H = A\frac{m_a^B(P_o - Pth)}{U W_t} + C \qquad (2.13)$$

where

m_a : mass flow rate of particles

U : traverse speed of the nozzle

W_t : the width of the kerf

P_o : operating pressure

A,B,C,Pth : coefficients determined by regression analysis

Work [27] employed particle kinetic energy to evaluate the depth of cut. This equation include operational parameters that are readily available, then all experimental results were substituted into equation to find a final model by the method of regression analysis. This equation demonstrates an acceptable accuracy. The correlation coefficients between predicted and observed data exceed 0.9. This model, However, does not include a number of process variables such as the material properties, the diameter of sapphire and water action. This work tried to improve the results presented in [27].

2.3 The Study of the Particle Motion in AWJ

The cutting results depend on slurry velocity that is the mean of water velocity and abrasive particle velocity. Because of the rather important role of particle during AWJ cutting, the particles motion was the principal subject of investigation. The motion of particles entrained in a stream of fluid has been investigated in a number of researches. Several equations were proposed for particles entrained in a_laminar flow. The forms of these equations depend on the forces considered in a particular study. Finnie [28] employed an equation governing the motion of particle subjected to the drag force This equation has the form:

$$\frac{4}{3}\pi r^3 \rho_p \frac{dv}{dt} = \frac{C_d}{2}\rho_a \pi r^2 (U-V)^2 \qquad (2.14)$$

where

r : particle radius

V : particle velocity

ρ_p : particle density

U : air velocity

ρ_a : air density

C_d : drag coefficient

Another form of the particle motion equation in a laminar flow and the applications are given in [29]. The various applications of this equation are discussed in [30-39].

The motion of particle in a turbulent flow was discussed , for example, in [40] Tchen [41] and Hjelmfelt [42] derived an equation of the motion of particles and discussed the particle response to the oscillatory motion of the carrying fluid. As a result of their work, the following equation was proposed:

$$\frac{\pi d^3}{6}\rho_p\frac{dU_p}{dt} = 3\pi\mu\rho_f d(U_f - U_p) + \frac{\pi d^3}{6}\rho_p\frac{dU_f}{dt} + \frac{\pi d^3}{6}\rho_f\left(\frac{dU_f}{dt} - \frac{dU_p}{dt}\right)$$

$$+\frac{3}{2}d^2\sqrt{\pi\rho_f\mu}\int_{t_o}^{t} dt'\frac{(dU_f/dt') - (dU_p/dt')}{t-t'} + F_e \qquad (2.15)$$

where

t_o : the starting time

index f : the fluid

index p : the particle

U : the velocity

d : the particle diameter

ρ : the density

F_e : external force

A numerical solution of this equation at various initial and boundary conditions is given is [43-48] .

The information about the motion of particles in the AWJ formed by conventional nozzle head is limited. Particularly, there is no direct determination of particle velocity, A simplified equation for the prediction of the particle velocity is given in [49]. Its derivation is based on the conservation of momentum. The equation is as given below:

$$V_{sw}\, m_w = (m_a + m_w)\, V_C$$

$$\frac{V_{sw}}{V_C} = \frac{1}{1 + m_a/m_w} \tag{2.16}$$

where

V_{sw} : the water velocity at the exit of sapphire orifice

V_C : the slurry velocity at the exit of carbide tube

m_a : the mass flow rate of abrasive

m_w : the mass flow rate of water

However, these model represents a mean slurry velocity in the mixing tube and can not be applied for evaluation of water and particle velocities. Another equation of particles motion is given in [50]. The following assumptions were made in the derivation.

1. Shape of particle is spherical.

2. Gravity and air resistance are small enough to be neglected.

3. The angle between the velocity vector and the longitudinal axis of the waterjet is relatively small.

Therefore, the velocity component in longitudinal direction was used to represent the velocity of waterjet. The final form of the equations proposed by Isobe are as follows:

$$\frac{d^2X}{dt^2}m + C_D\left(\frac{dX}{dt}\right)^2\frac{\rho\pi R^2}{2} = 0 \tag{2.17}$$

$$\frac{d^2X}{dt^2}m + C_L\left(\frac{dX}{dt}\right)^2\frac{\rho\pi R^2}{2} = 0 \tag{2.18}$$

where

x : longitudinal coordinate

y : transversal coordinate

R : radius of particle

ρ : density of particle

m : mass of particle

C_D : drag coefficient

C_L : lift coefficient

The above equation does not consider the energy dissipation in the turbulent flow that is an important factor in the determination of AWJ behavior. Also, the effects of interaction between particles have been neglected in this derivation.

In addition to the above model, Isobe also obtained the average velocity of abrasive particles by counting the numbers of the impact craters on an aluminum plate, which he used as a test piece, However, the obtained velocity may present the velocity of the particle on the periphery of the jet and the accuracy of the results is strongly correlated to the counting method.

Chen [51] used LTA (Laser Transit Anemometer) to measure the velocity of the waterjet and the velocity of slurry in AWJ up to 345 MPa of water pressure. A regression equation that correlated the results of velocity measurement with the operating parameters has been constructed. This regression equation has a form:

$$\frac{V_{cw} - V_a}{V_{sw}} = 0.627\left(\frac{Q_a}{Q_w}\right)^{2.557\left(\frac{D_o}{D_t}\right)^2} \tag{2.19}$$

where

V_a : velocity of abrasive particles

V_{cw} : velocity of pure waterjet at the exit of focusing tube

V_{sw} : velocity of pure water jet at the exit of sapphire

Q_a : volume flow rate of abrasive particles

Q_W : volume flow rate of water

D_o : diameter of sapphire

D_t : diameter of focusing tube

Chen reported that correlation coefficient for above equation is 0.926. He applied almost all operating parameters to his equation. So, his equation is easy to be used in the industrial condition although the form of the equation needs to be further improved.

2.4 Comments on the Survey

1. The optimal way of mathematical modeling on AWJ machining is the use of semi-empirical model that possesses physical sense and statistically satisfies experimental results.

2. Almost all of prediction of cutting results were focused on the particle action while water action was usually omitted.

3. Although several investigations of the momentum transformation from water to abrasive particles after being mixed have been reported. No satisfactory answers to description of transformation. Particularly, so far, the velocities of water and abrasive at the exit of mixing tube.

4. The published prediction technique for AWJ machining results is still not adequate for practical use are not defined sufficiently.

CHAPTER 3

KNOWLEDGE OF REGRESSION ANALYSIS

Regression analysis is a statistical technique for developing a quantitative relationship between a dependent and one or more independent variables. It utilizes experimental data on the pertinent variables to develop a numerical relationship showing the influence of the independent variables on a dependent variable of the system.

Regression can be applied to correlating data in a wide variety of problems ranging from the simple correlation of physical properties to the analysis of a complex industrial system. If there is no previous information about the relationship among the pertinent variables, the form of the equation can be assumed and fitted to experimental data on the system.

Frequently a linear function is used for such an assumption. If a linear function does not fit the experimental data properly, the use of nonlinear functions should be explored.

3.1 Simple Linear Regression

In the simplest case the proposed functional relationship between two variables is

$$Y = \beta_0 + \beta_1 X + \varepsilon \tag{3.1}$$

In this model Y is the dependent variable, X is the independent variable, and ε is a random error (or residual) which is the amount of variation in Y not accounted for by the linear relationship. The parameters β_0 and β_1 are called the regression coefficients which are unknown and are to be estimated. Usually X is not a random variable but should take fixed value. It is assumed that the errors ε are independent and have a normal distribution with

mean 0 and variance σ^2, regardless of what fixed value of X is being considered. Taking the expectation of both sides of eq (3.1), we have

$$E(Y) = \beta_0 + \beta_1 X = E(Y/X) \tag{3.2}$$

where the expected value of the errors is zero. E(Y/X) is called the regression of Y on X .

In order to estimate the relationship between Y and X we have n observations on Y and X, denoted by (X_1,Y_1), (X_2,Y_2),... (X_n,Y_n). by eqs.(3.1) and (3.2) we can write the assumed relationship between Y and X as

$$Y = E(Y/X) + \varepsilon \tag{3.3}$$

The aim of the computation is to estimate β_0 and β_1 and thus E(Y/X) or Y in terms of the n observation, the values X_1, X_2,...Xn, and corresponding Y_1, Y_2,...Y_n. If $\hat{\beta}_0$ and $\hat{\beta}_1$ denote estimates of β_0 and β_1, then an estimate of E(Y/X) is denoted by $\hat{Y} = \hat{E}(Y) = \hat{\beta}_0 + \hat{\beta}_1 X$ Thus each observed Y_i can be written as

$$Y_i = \hat{Y}_i + e_i \qquad\qquad i=1,2,\bullet\bullet\bullet,n,$$

where $\hat{Y}_i$ is the estimate of $E(Y_i)$ and e_i is the estimate of ε_i. Therefore, E(Y) has a linear relationship:

$$Y_i = \beta_0 + \beta_1 X_i + \varepsilon_i = \hat{\beta}_0 + \hat{\beta}_1 X_i + e_i \qquad i = 1,2,\bullet\bullet\bullet,n, \tag{3.4}$$

The observed residual e_i is $Y_i - \hat{Y}_i$ which is the difference between the observed Y_i and the estimated $\hat{Y}_i = \hat{\beta}_o + \hat{\beta}_1 X_i$. The quantity $\hat{Y} = \hat{\beta}_o + \hat{\beta}_1 X$ is commonly called the predicted value of Y resulting from the estimated regression line.

The problem is now to obtain estimates $\hat{\beta}_o$ and $\hat{\beta}_1$ from the sample for the unknown parameters β_o and β_1. This can best be done by the least squares method. This method minimizes the sum of least squares, $\sum_{i=1}^{n} e_i^2 = SS_E$, of the differences between the predicted values and the experimental values for the dependent variable. The method is based on the principle that the best estimation of β_o and β_1 are those that minimize the sum of squares due to error, SS_E. The error sum of squares is

$$SS_E = \sum_{i=1}^{n} e_i^2 = \sum_{i=1}^{n} \left(Y_i - \hat{Y}_i \right)^2 = \sum_{i=1}^{n} \left(Y_i - \hat{\beta}_o - \hat{\beta}_1 X_i \right)^2 \tag{3.5}$$

To determine the minimum of SS_E, the partial derivative of the error sum of squares with respect to each constant ($\hat{\beta}_o$ and $\hat{\beta}_1$ for this model) is set equal to zero to yield.

$$\frac{\partial (SS_E)}{\partial \hat{\beta}_o} = \frac{\partial}{\partial \hat{\beta}_o} \left(\sum_{i=1}^{n} \left(Y_i - \hat{\beta}_o - \hat{\beta}_1 X_i \right)^2 \right) = 0 \tag{3.6}$$

$$\frac{\partial (SS_E)}{\partial \hat{\beta}_o} = \frac{\partial}{\partial \hat{\beta}_1} \left(\sum_{i=1}^{n} \left(Y_i - \hat{\beta}_o - \hat{\beta}_1 X_i \right)^2 \right) = 0 \tag{3.7}$$

Carrying out the differentiation, we obtain finally:

$$\hat{\beta}_1 = \frac{\left(\sum_{i=1}^{n} X_i Y_i - n\overline{X}\,\overline{Y}\right)}{\sum_{i=1}^{n}\left(X_i^2 - n\overline{X}^2\right)} \tag{3.8}$$

$$\hat{\beta}_o = \overline{Y} - \hat{\beta}_1 \overline{X} \tag{3.9}$$

where $\overline{X}$ and $\overline{Y}$ are the average of X_i and Y_i, respectively. regression equation or eq(3.1) is:

$$\hat{Y} = \hat{\beta}_o + \hat{\beta}_1 X \tag{3.10}$$

The practical meaning of all parameters is showed in Fig 4.

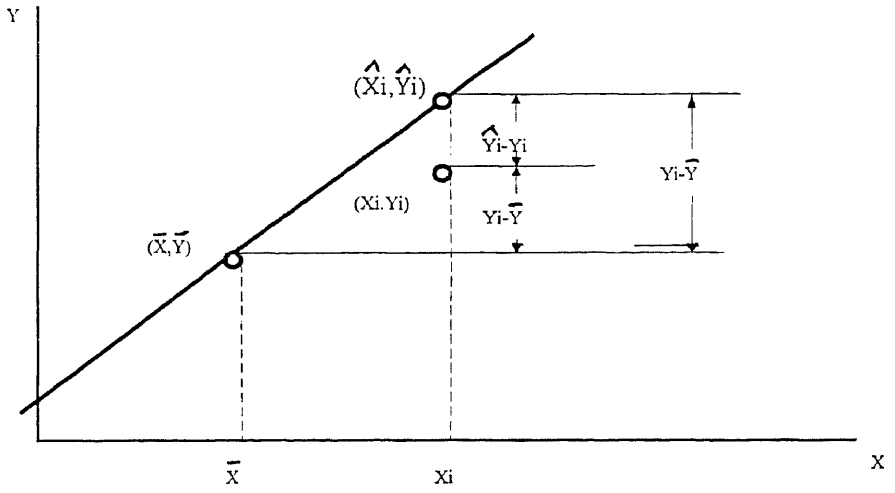

Figure 4 Partitioning of Total Sum of Squares in Simple Linear Regression

3.2 Multiple Linear Regression

In last section, we consider the case where only one independent variable was allowed in the regression model. Now we consider the case in which two or more independent variables are allowed:

$$Y = \beta_o + \beta_1 X_1 + \beta_2 X_2 + \cdots + \beta_p X_p + \varepsilon \tag{3.11}$$

Matrix algebra is readily adaptable to multiple linear regression for eq (3.11). The assumptions are the same as for the simple linear model except that now we have p independent variables, To obtain the least squares estimates for the β_i, we must again minimize the error sum of squares, As with simple linear regression, we have n observations on $Y, X_1, X_2 \ldots X_p$, and the error sum of squares is

$$SS_E = \sum_i e_i^2 = \sum_i \left(Y_i - \hat{Y}_i \right)^2 = \sum_i \left(Y_i - \hat{\beta}_0 - \hat{\beta}_1 X_{1i} - \hat{\beta}_2 X_{2i} - \cdots - \hat{\beta}_p X_{pi} \right)^2 \tag{3.12}$$

which is minimized by setting $\partial(SS_E) \big/ \partial \hat{\beta}_i = 0$ to get the system of normal equations as follows:

$$\begin{aligned}
&n\hat{\beta}_o + \hat{\beta}_1 \Sigma X_{1i} + \hat{\beta}_2 \Sigma X_{2i} + \cdots + \hat{\beta}_p \Sigma X_{pi} = \Sigma Y, \\
&\hat{\beta}_o \Sigma X_{1i} + \hat{\beta}_1 \Sigma X_{1i}^2 + \hat{\beta}_2 \Sigma X_{1i} X_{2i} + \ldots + \hat{\beta}_p \Sigma X_{1i} X_{pi} = \Sigma X_{1i} Y_i, \\
&\quad \vdots \qquad\qquad \vdots \qquad\qquad \vdots \\
&\quad \vdots \qquad\qquad \vdots \qquad\qquad \vdots \\
&\hat{\beta}_o \Sigma X_{pi} + \hat{\beta}_1 \Sigma X_{1p} X_{pi} + \hat{\beta}_2 \Sigma X_{2i} X_{pi} + \ldots + \hat{\beta}_p \Sigma X_{pi}^2 = \Sigma X_{pi} Y_i,
\end{aligned} \tag{3.13}$$

where all the summations go from i=1 to i=n. To obtain the estimates $\hat{\beta}_o, \hat{\beta}_1, \ldots \hat{\beta}_p$ one needs to solve the system (3.13) of P+1 linear equations for the unknown $\hat{\beta}_o, \hat{\beta}_1, \ldots, \hat{\beta}_p$. In the simple linear case we had two equations in two unknown. A much easier approach to the normal equation is found from matrix algebra:

$$\beta = \left(X^t X\right)^{-1} X^t Y \tag{3.14}$$

3.3 Nonlinear Regression

It probably comes as no surprise that possible nonlinear mathematical relationships between the variables X and Y can be transformed to linear relationships in two new variables by applying relatively simple mathematical operations to the original nonlinear form. A nonlinear model which occurs quite frequently is

$$Y = \beta_o e^{\beta X} \tag{3.15}$$

The model is usually handled by means of taking the natural log of both sides of the equations yielding:

$$\ln Y = \ln \beta_o + \beta_1 X \tag{3.16}$$

letting $Z = \ln Y, \alpha_o = \ln \beta_o$, and $\alpha_1 = \beta_1$, the model thus reduces to the linear model :

$$Z = \alpha_o + \alpha_1 X \tag{3.17}$$

using the above linear model, estimates $\hat{\alpha}_o$ and $\hat{\alpha}_1$ are obtained. From these one obtains the estimates $e^{\hat{\alpha}_o}$ and $\hat{\alpha}_1$ for β_o and β_1. We also can apply this method to the other form of nonlinear equations and just first linearizing and then doing the least squares estimation (see Table 1).

Function	Equation	Transformed Equation
Hyperbolic	$Y = \frac{X}{\beta_0 X + \beta_1}$	$\frac{1}{Y} = \beta_0 + \beta_1 \frac{1}{X}$
Exponential	$Y = \beta_0 e^{\beta_1 X}$	$\ln Y = \ln \beta_0 + \beta_1 X$
Power	$Y = \beta_0 X^{\beta_1}$	$\ln Y = \ln \beta_0 + \beta_1 \ln X$
Logarithmic	$Y = \beta_0 + \beta_1 \ln X$	$Y = \beta_0 + \beta_1 \ln X$
Inverse Exponential	$Y = \beta_0 e^{\frac{\beta_1}{X}}$	$\ln Y = \ln \beta_0 + \frac{\beta_1}{X}$
Pseudo-Exponential	$Y = \frac{1}{\beta_0 + \beta_1 e^{-x}}$	$\frac{1}{Y} = \beta_0 + \beta_1 e^{-x}$

table 1 Nonlinear Equations and Their Simple Linear Transforms

One should be careful using the transformations such as the above, since if it is assumed that the original variable is normally distributed, then the transformed variable may not be. The homogeneity of variance property may be likewise violated. Frequently, however, the original assumption of normality may not be justified and the transformed variables have a distribution close to normal.

3.4 Correlation Analysis

Having determined the relationship existing between variables, the next question which arises is how closely the variables are associated. The statistical techniques which have been developed to measure the degree of association between variables are called correlation methods. A statistical analysis performed to determine the degree of correlation is called a correlation analysis. The term used to measure correlation is referred to as a correlation coefficient, The correlation coefficient measures how well the regression equation fits the experimental data. As such, it is closely related to the standard error of estimate, $\hat{\sigma}$.

(1) Correlation Coefficient R

The correlation coefficient R should exhibit two characteristics:

(a) It should be large when the variables are closely associated and small when there is the association is weak.

(b) It must be independent of the units used to measure the variables.

An effective correlation coefficient which exhibits these two features is the square root of the fraction of the sum of squares of derivations of the original data from the regression curve that has been accounted for by the regression. This is a justifiable definition since the closeness of the regression curve to the data points is reflected in how much of the total corrected sum of squares, SS_T, is accounted for by the sum of squares due to regression, SS_R. We have the equation:

$$\Sigma\left(Y_i-\bar{y}\right)^2=\Sigma\left(Y_i-\hat{Y}_i\right)^2+\Sigma\left(\hat{Y}_i-\bar{Y}\right)^2 \qquad [\ SS_T=SS_E+SS_R\ ] \qquad (3.18)$$

In view of this we define the correlation coefficient in terms of the proportional reduction in the sum of squares accounted for by the regression of y on x. The precise definition is

$$R^2=SS_R/SS_T=(SS_T-SS_E)/SS_T=1-SS_E/SS_T \qquad (3.19)$$

As $SS_E \le SS_T$, R^2 lies between 0 and 1. If the regression curve is a poor fit of the experimental data, R^2 is close to zero. After derivation, R^2 for a simple linear regression is

$$R^2 = \frac{\left[\Sigma(X_i-\overline{X})(Y_i-\overline{Y})\right]^2}{\Sigma(X_i-\overline{X})^2\Sigma(Y_i-\overline{Y})^2} \tag{3.20}$$

for the multiple linear regression R^2 is

$$R^2 = \frac{\hat{\beta}\,\Sigma(X_{1i}-\overline{X})(Y_i-\overline{Y})+\ldots+\hat{\beta}_p\Sigma(X_{pi}-\overline{X})(Y_i-\overline{Y})}{\Sigma(Y_i-\overline{Y})^2} \tag{3.21}$$

(2). Sample Variance

$$S_y^2 = \frac{\Sigma(Y_i-\overline{Y})^2}{n-1} = \frac{SS_T}{n-1} \tag{3.22}$$

is the unconditional sample variance of y.

$$S_{y/x}^2 = \frac{\Sigma\left(Y_i-\hat{Y}_i\right)^2}{n-2} = \frac{SS_E}{n-2} \tag{3.23}$$

is the conditional value of the sample variance of y given knowledge of the associated paired values of x. It is the best estimate of the true but unknown value of σ^2.

(3). Sample Covariance $\mathrm{cov}(X_1, X_2)$

The definition of S_{xy} is as follows:

$$\mathrm{cov}(X_1, X_2) = E\{(X_1-\mu_1)(X_2-\mu_2)\} = E\{X_1X_2\}-\mu_1\mu_2 \tag{3.24}$$

Transformed:

$$\mathrm{cov}(X_1, X_2) = E(X_1 X_2) - E(X_1)E(X_2) \tag{3.25}$$

The covariance is a measure of the relationship that exists between X_1 and X_2. If X_1 and X_2 are statistically completely independent random variables, $E(X_1 X_2) = E(X_1)E(X_2)$. This implies that the covariance of statistically independent random variables is zero. Because of the units of measure for the covariance, it is often convenient to have a dimensionless form of the covariance. One such form is the correlation coefficient between X_1 and X_2 defined as :

$$\rho = \mathrm{corr}(X_1, X_2) = \frac{\mathrm{cov}(X_1, X_2)}{\sqrt{S_{x1} S_{y1}}} \tag{3.26}$$

where S_{X_1} and S_{X_2} are the variance of X_1 and X_2, respectively. The correlation coefficient is bounded between -1 and +1. If ρ is small, X_1 and X_2 are independent. If ρ has middle value, say, $0.3 \le \rho \le 0.7$, there are some correlation existing between X_1 and X_2, but it is weak. If ρ is in the high value, say, $\rho \ge 0.8$, we may think that strong correlation exists between X_1 and X_2.

(4) Sample Residuals

The sample residuals is defined as $e_i = Y_i - \hat{Y}_i$. One purpose of studying the e_i is to determine whether the assumption that the ε_i is distributed $N(0, \sigma_{y/x})$ is satisfied. If this assumption is not satisfied, at least in a "robust" sense, then we are no longer assured that the estimates of β_o and β_1 are minimum variance unbiased estimates. Further, all the confidence intervals and the joint confidence region are no longer valid, If the assumption

of normality is true, the $r_i = \frac{\varepsilon_i}{\sigma_{y/x}}$ which are approximated by the $g_i = \frac{e_i}{S_{y/x}}$, are distributed $N(0,1)$, where r_i is the i^{th} standardized residual.

The residuals from a regression fit should be plotted on an ordinary scale against various quantities relevant to the phenomenon and the data. A non exhaustive set of such plots might be to plot the residuals against input order, independent variable, dependent variable and the fitted values of dependent variable as yielded from the model. The idea behind this type of plot is to search for evidence of non random trends or tendencies in the residuals. If the fit is adequate and the assumptions that we have made earlier are satisfied, we would expect an even band to be exhibited by the plot. An example of such a plot with an even band is given in Fig 5.

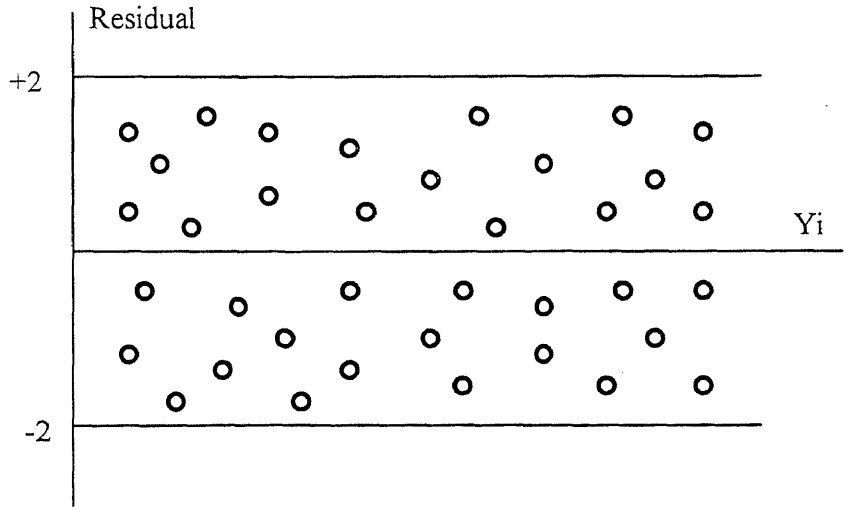

Figure 5 A Residual Plot with an Even Random Band

CHAPTER 4

AWJ APPARATUS AND EXPERIMENTS

The purpose of this study is to established a mathematical model which will improve existing models relating the depth of AWJ cutting with process variable. The experimental data is acquired in the course of the performed experiments. In this chapter experiments and AWJ machining apparatus will be briefly described in order to outline the principal features of the data acquisition.

The objectives of performed experiments were the study of the effect of processing parameters of AWJ on the material machining results and to construct the prediction model. An industrial scale abrasive waterjet cutting system was employed for machining tests and an analyser "Videomatrix" was used for machining results measurement. The experimental facilities, samples preparation, the test matrices, the measurement instruments and experimental procedure are described in the following sections. (All figures in this chapter were from work [27])

4.1 Experimental Facilities

The abrasive waterjet cutting system used in this study was manufactured by the Ingersoll-Rand. The system (Fig 6) xonsists of the units described below.

4.1.1 Water Preparation Unit

The major components of this unit are the booster pump, filters, water softener, prime mover, intensifier, accumulator, control and safety instrumentation. The major functions of the unit is to feed continuously pure water pressurized to the required pressure. To ensure continuous flow into a high pressure cylinder, a booster pump supplies water into a low pressure water circuit (180 psi). Iron and calcium compounds contained in the water tend to come out of the solution at high pressure and damage the

softener are used. This pump design also enables us to add polymer additives to the water and blends the water and polymers.

A hydraulically driven (10-40 hp) oil intensifier is the most important part of the system. It develops pressure up to 408 MPa in the water from the booster pump. There are two separate circuits for oil pressure of about 20.4 MPa developed by a rotary pump used to drive an intensifier. The intensifier is a double acting reciprocating (152.4 mm diameter) type pump.

The high pressure emergency damp valve is a rapid acting two way position valve used to turn the jet ON or OFF in response to control commands. The high pressure water from both sides of the intensifier is discharged to an accumulator where the pressure is stabilized. Since the compressibility of the water at 374 MPa is 12 percent ,water is not discharged uniformly from intensifier at various piston positions. Thus, the accumulator is needed to provide uniform discharge pressure and flow.

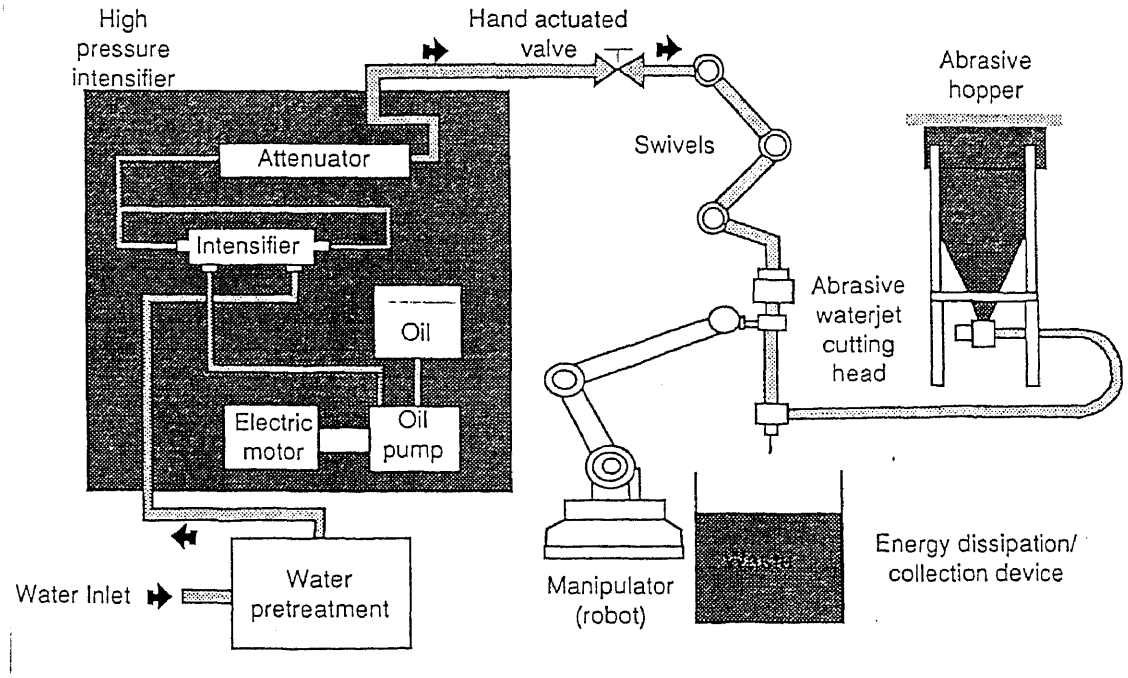

Figure 6 AWJ Machining System

4.1.2 High Pressure Water Distribution System

The output from the accumulator, the high pressure water, is carried away to the work station through a series of high strength pipes, swivels, flexible joints, and fittings. A hose can be used to eliminate the need for swivels. The number of joints, elbows, and the total pipe length determine the line pressure drop. The principal advantage of the distribution system is centralized water preparation unit for several work stations, located at different suitable places for different applications.

4.1.3 Work Station

It is the place where actual cutting operation is performed. It can be of variety of types located at different places depending on application. The work station used in this study is described below.

4.1.3.1 Robotic Work Cell

The gantry CNC 5-axis robotic work cell shown in Fig 7 is controlled by the Allen-Bradley 8200R controller (Fig 8).

The controller contains the following standard features:

-Simultaneous continuous path control of all axes

-Linear interpolation

-Circular interpolation

-Digital readout for all axes

-Incremental feed for all axes

-Jog control for all axes

-Inch/metric switchable input

-Absolute/incremental input

-Manual data input

-Sequence number search/display

-Feedrate override

-Edit lookout

-Multiple part storage and edit

-Memory retention during power outage

-Dry run function

-Tool life timer

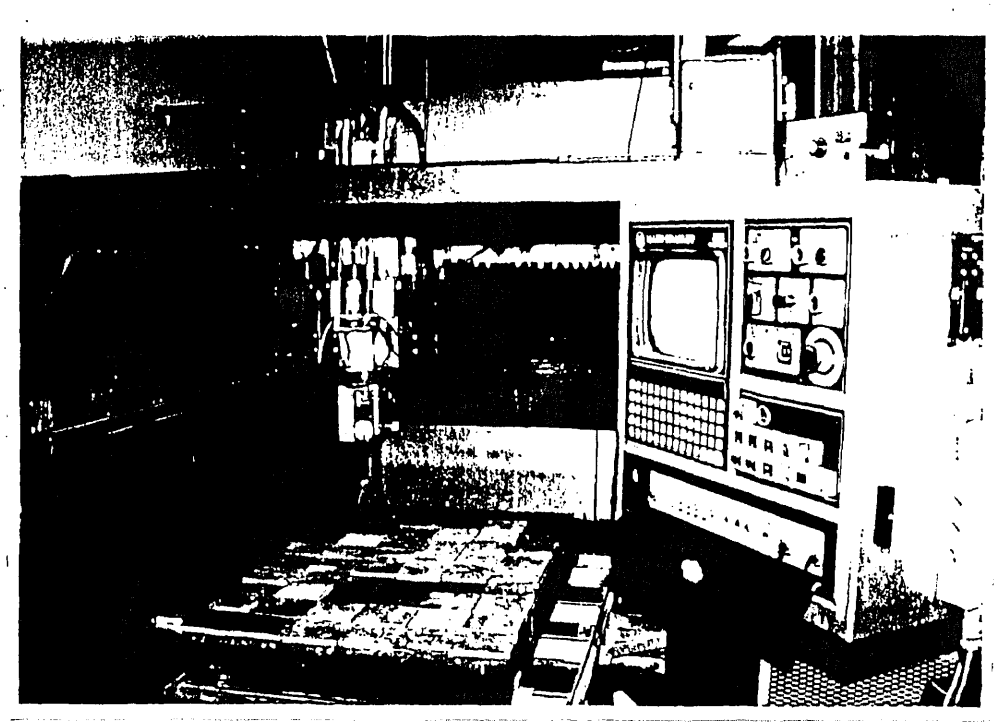

Figure 7 The Gantry CNC 5-axis Robotic Work Cell

The controller is capable of receiving input from keyboard entry, punched tape, and/or magnetic tape in accordance with EIA standards RS-232, 244, 358 and 274. Standard G, F and M codes are utilized.

4.1.3.2 Abrasive Feeder

In the abrasive feeding system (Fig 9), the bulk abrasive is stored in a larger hopper whose exit is located on an electronically controlled vibrating tray. Through the control of

the amplitude of vibration, the tray meters the flow of abrasive to a hopper. It is then aspirated through a short section of a flexible tube into the mixing chamber of the nozzle body.

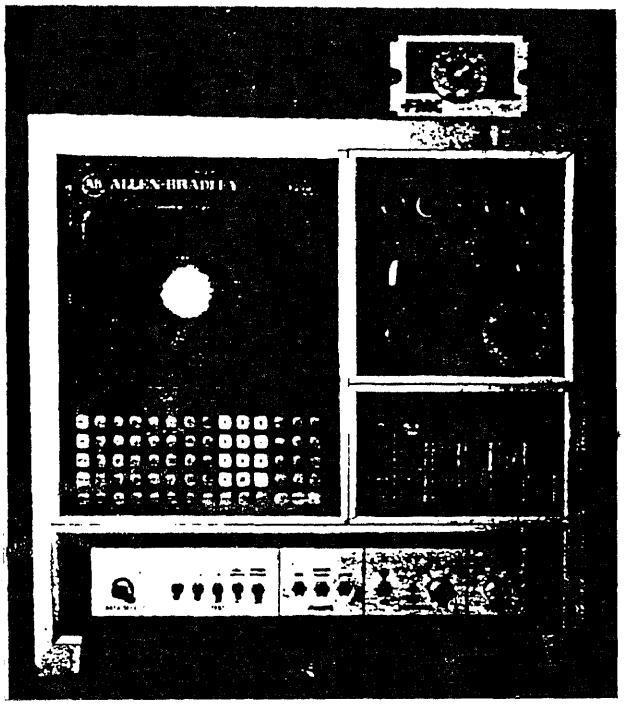

Figure 8 The Allen-Brandley 8200R Controller

4.1.3.3 Catcher System

The catcher tank (Fig 10) installed below the suspended cutting head collects the spent abrasive, the water and the cutting debris, which settle to the bottom of the tank. The size of the tank enables us to contain the noise of the high pressure jet. A drain near the base of the catcher tank is provided. Through the drain, the water and the abrasive flow into a settlement tank where the water drains out and the abrasive grit settles down. The grit is disposed of periodically from the tank.

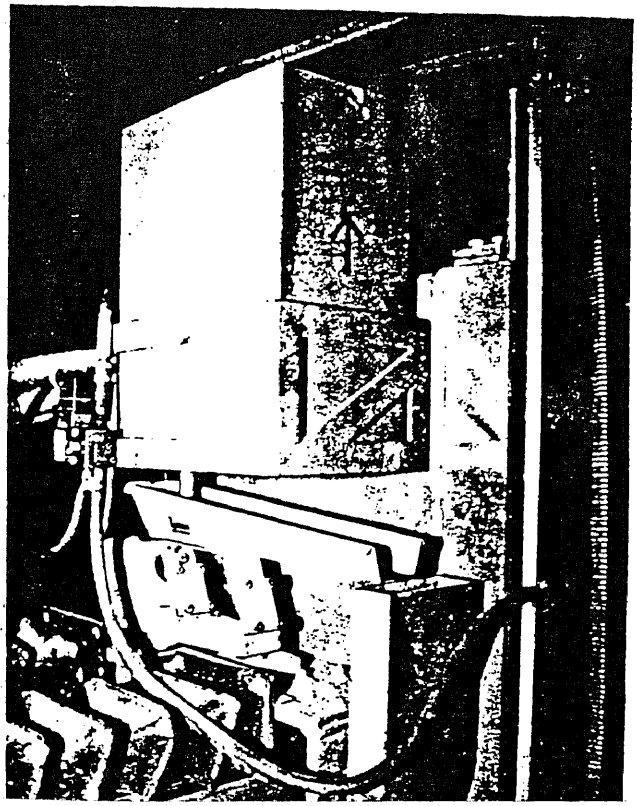

Figure 9 Abrasive Feeder

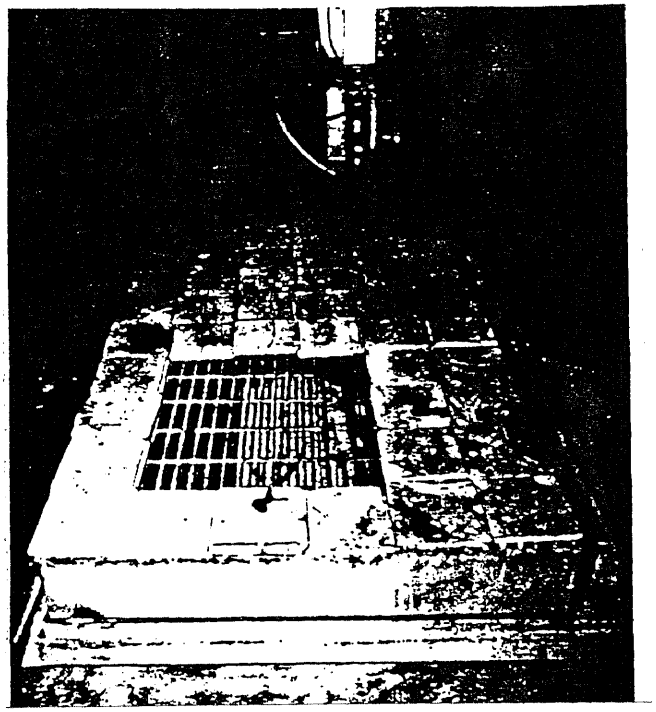

Figure 10 Catcher System

4.2 Measurement Instrument

A Matrix Videometrix Econoscope is used for the measurement of experimental results such as the depth of cut and the width of kerf. This instrument is a fully automatic, 3-D video inspection system. It uses non contact technique to provide rapid dimensional verification of complete parts or specified features of a part.

The Econoscope comprises a General Purpose Computer, a 3-axis Positioning Control System, a Digital Image Processor and part Monitor Section. Specifically designed to be easy for use, the Econoscope operates at a high speed. producing very accurate (with resolution up to 0.1 micron) and repeatable results. The software is menu/prompt driven so the operator need not learn cumbersome computer language.

4.3 Experimental Procedures

The machining experiments were conducted under the following prudential considerations:

1) The workcell was always in normal conditions during experiments.

2) All experiments were carried out by one person who trained to operate the workcell..

3) Experimental setups were at the similar conditions of the whole experiments.

4) Measurement instruments were always fine tuned in normal conditions.

5) Measurements were conducted by the same person who carried out the experiments so that the experimental results were collected in the consistent situation.

4.3.1 Samples Preparation

In the course of experiments the samples of steel AISI 1018, aluminum Al 6061-T6 and titanium Gr-2 have been used. The chemical compositions and mechanical properties of these materials are listed in Table 1 and 2, respectively.

Material	Compositions					
Al 6061-T6	% Mg	% Si	% Cr	%Cu	%Al	
	1.0	0.6	0.2	0.27	97.93	
AISI 1018	% C	% Mn	% P	% S	% Fe	
	0.15-0.2	0.6-0.9	0.4	0.05max	remainder	
Ti Gr2	% N	% C	% H	% Fe	$\% O_2$	% Ti
	0.03	0.1 max	0.015max	0.3max	0.25max	remainder

Table 2 Chemical Compositions of Experimental Materials

	Tensile Strengt (MPa)	Yield Strength (MPa)	Elongation (%in 2 in.)	Vickers Hardness(HV)	Flow Strength(MPa)
Al 6061-T6	310	275	12	111	293
AISI 1018	450	380	16	131	415
Ti Gr2	345	275	20		310

Table 3 Mechanical Properties of Experimental Materials

4.3.2 Experimental Data

All experiments were conducted on three different kinds of ductile materials (steel, aluminum, and titanium) with three types of sizes of abrasive particle (50mesh, 80mesh, 220mesh) and every combination of the experiment was done at least three times which satisfied the statistical requirements for the sample size. So, total number of the experiments is over 1000. The measured results of cutting experiments include depth of cut, top kerf width and bottom kerf width. All the data are listed in Appendix.

CHAPTER 5

A MATHEMATICAL MODEL FOR PREDICTION OF DEPTH OF CUT

AWJ has been a powerful cutting tool as a new manufacturing technique since it was developed. A practical prediction technique relating process conditions and results is a necessary for the technology utilization. Empirical method is a direct approach for development of a prediction technique of AWJ machining process, but it is also a blind approach. The theoretical method, Hashish's model, which is established according to the physical relationship and has a physical sense, usually contains parameters which are not readily available at industrial conditions. The balanced way, the semi-empirical method, like Chung's model. Such method used by Chung was constructed on the base of the energy balance of cutting. Moreover, the Chung's analysis does not included all important process variables such as material properties and sapphire diameter.

This study is an extension of the Chung's work by the inclusion of new variables and the actions of water.

5.1 The Idea for the New Model

In constructing the new model, three steps were undertaken. The first step involved development of a theoretical model which included main operating parameters, material properties, and water and particle actions. Then, the theoretical model was improved by the statistical analysis of the acquired data. The last step included the construction of the regression model, which conformed to the results of cutting experiments.

In order to simplify the model, the work was limited to cutting of steel AISI 1018 at the particles size of mesh 80. By the changes of the regression coefficient the model can be applied to different material and sizes of particle.

Three statistical criteria were used to assess the fitted equation synthetically:

(1) multiple correlation coefficient R^2 (the higher R^2 value, the better the fitting)

(2) the number of $g_i > \pm 2\%$ (the lower the g_i value, the better the fitting)

(3) the plot of standard residual $g_i = \frac{Y_i - \hat{Y}_i}{S_{y/x}}$ (the more even the plot, the better the fitting)

5.2 A Theoretical Model

AWJ machining is a complicated process. So far, it is not clear how the particle moves in the nozzle and how the particles are distributed during the cutting, In order to investigate the relationship between depth of cut and particle motion effectively, it is natural to study the variation of particle velocity at the macroscopic level, rather than at the microscopic level. Because of this, we are mostly concern with velocity distribution at the nozzle exit rather than the velocity in the nozzle. The regression analysis is used to investigate mean values of key elements of the process.

5.2.1 Energy Conservation Equation

It is assumed that in the course of the cutting (Fig 11), only the kinetic energy changes and while kinds of internal energy and potential energy are constant. Secondly, the workpiece damage occurs only due to the compressive stress induced by the particles stream. Then from (Fig11) we have the following relationship determined by the kinetic energy conservation:

work done by cutting of part B = kinetic energy at the exit of the nozzle of part A

work done by AWJ = water kinetic energy + particle kinetic energy

$$W = E_w + E_a$$

where

$$W = \text{cutting force} \times \text{depth of cut} = \sigma W_t u H \times 10^{-3} \qquad (N \cdot m/min)$$

$$E_w = \frac{1}{2} m_w V_{cw}^2 \qquad \text{at the exit of carbide tube} \qquad (N \cdot m/min)$$

$$E_a = \frac{1}{2} m_a V_a^2 \qquad \text{at the exit of carbide tube} \qquad (N \cdot m/min)$$

$$m_w = \left(\frac{1}{4}\pi D_o^2\right) V_{sw} \rho_w = 15\pi D_o^2 V_{sw} \qquad (g/min)$$

Then, we have:

$$\sigma W_t u H \times 10^{-3} = \frac{1}{2}\left(15\pi D_o^2 V_{sw}\right) V_{cw}^2 + \frac{1}{2} m_a V_a^2$$

$$\sigma W_t u H = 7500 D_o^2 \cdot V_{sw} \cdot V_{cw}^2 + 500 m_a V_a^2 \qquad (5.1)$$

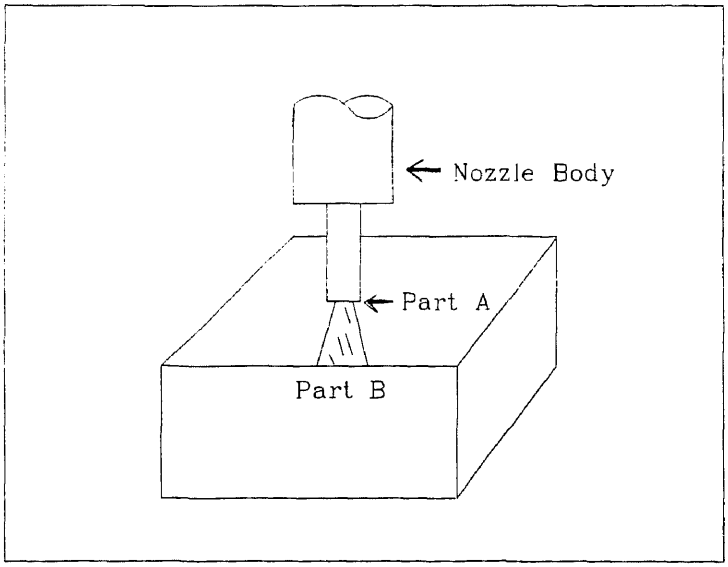

Figure 11 The Schematic of Cutting by the AWJ

5.2.2 Velocities of Water and Abrasive at the Exit of the Tube

According to the momentum balance of water and abrasive, we obtain a simple equation of slurry velocity:

$$V_m = \frac{m_w}{m_w + m_a} V_{sw}$$

$$V_m = \frac{1}{1 + \frac{m_a}{m_w}} V_{sw} \tag{5.2}$$

From eq (5.2) it follows that $V_a < V_m < V_{cw}$. In order to simplify the derivation, it is set that $V_{cw} = V_m$, and C_a is added into equation for V_m to form an equation for V_a which accounts for the effects of abrasive size and collision efficiency among water, abrasive and tube wall on the V_a

$$V_{sw} = \sqrt{\frac{2P_o}{\rho_w}} \tag{5.3}$$

$$V_m = \frac{1}{1 + \frac{m_a}{m_w}} V_{sw} = \frac{1}{1 + \frac{m_a}{2107.4 D_o^2 P_o^{1/2}}} V_{sw} \tag{5.4}$$

$$V_a = \frac{1}{1 + \frac{C_a m_a}{m_w}} V_{sw} = \frac{1}{1 + \frac{C_a m_a}{2107.4 D_o^2 P_o^{1/2}}} V_{sw} \tag{5.5}$$

5.2.3 The Theoretical Model

Substituting eqs (5.3), (5.4) and (5.5) into eq (5.1) we receive:

$$\sigma W_t uH = 7500\pi D_o^2 \cdot \sqrt{\frac{2P_o}{\rho_w}} \cdot \frac{\frac{2P_o}{\rho_w}}{\left(1+\frac{m_a}{2107.4D_o^2P_o^{1/2}}\right)^2} + \frac{1}{2}m_a \frac{\frac{2P_o}{\rho_w}}{\left(1+\frac{C_a m_a}{2107.4D_o^2P_o^{1/2}}\right)^2}$$

Arranging above equation , we obtain the following model:

$$H = C_1 \frac{D_o^2 P_o^{3/2} K_w^2}{\sigma W_t u} + C_2 \frac{m_a P_o K_a^2}{\sigma W_t u} \qquad (5.6)$$

(A) (B)

where

$$C_1 = 15000\sqrt{2}\pi\sqrt{\rho_w}$$

$$C_2 = \frac{1}{\rho_w}$$

$$K_w = \frac{1}{1+\frac{m_a}{2107.4D_o^2P_o^{1/2}}}$$

$$K_a = \frac{1}{1+\frac{C\ m_a}{2107.4D_o^2P_o^{1/2}}}$$

From (5.6) it is apparent that the part A represents the depth of penetration due to the water action, which part B represents the depth of penetration caused by abrasive action.

5.3 An Improved Model

The objective of this section is to improve the theoretical model in terms of (a) the correlation between depth of cut and operating parameters acquired by the previous typical researches, (b) the interaction between water action and abrasive action, and (c) correlation among the independent variables.

5.3.1 Relationship Between Depth of Cut and Individual Operating Parameters

Now let's review some typical results relating depth of cut with individual operating parameters, obtained by Chung. Figure 12-15 show that the depth of cut is inversely proportional to the traverse rate (Fig 12), but it is proportional to the pressure P_o(Fig 14) and the ratio of sapphire diameter over carbide diameter. The relationship between H and m_a can be approximated by a polynomial curve (Fig 13) because the fraction of particles sufficiently accelerated by the water stream is reduced as the total amount of particles increase. beyond a specific level, further increase in the abrasive flow rate does not effect machining results. So, it is necessary to change m_a in eq (5.6) into m_a^A so as to tally with the experimental results.

5.3.2 Correlation among the Operating Parameters

Total 150 data of steel AISI 1018 with particle size 80 mesh was used for statistical evaluation of correlation among independent variables. Table 4 illustrated correlation coefficients between individual parameters from which we can conclude:

(1) Correlation coefficient between individual parameters are under 0.34. It means that the operating parameters are independent. This allowed us to carry out the regression analysis for the model construction.

(2) Correlation coefficient $\rho_{W_t D_t}$ between W_t and D_t is 0.933 which allow us to substitute W_t with D_t^B.

5.3.3 Interaction Between Water Action and Abrasive Action

Let's set for eq(5.6) as:

(1). $H_w = \frac{D_o^2 P_o^{3/2} K_w^2}{\sigma D_t^B u}$ (water action) , $H_a = \frac{m_a^A P_o K_a^2}{\sigma D_t^B u}$ (particle action)

(2). A=B=1,

(3). $\frac{2107.4}{C_a} = 550$

From the regression analysis for eq (5.6), we found the correlation coefficient between H_a and H_w $\rho_{Ha,Hw}$=0.917. This indicates existence of interaction between H_a and H_w. Therefore, a general equation for the evaluation of H can be given in the form of:

$$H = C_1 H_w + C_2 H_a + C_3 H_w H_a + C_4 H_w^2 H_a + C_5 H_w H_a^2 + C_6 H_w^2 H_a^2 + \ldots + C_o \qquad (5.7)$$

The coefficients C_n determined by regression analysis are given in table 5. From table 5 it is obvious that the regression equation can be reduced to the form $H = C_1 H_w + C_2 H_a + C_3 H_w H_a + C_o$ Substituting expression for H_a and H_w we obtain:

$$H = C_1\left(\frac{D_o^2 P_o^{3/2} K_w^2}{\sigma D_t^B u}\right) + C_2\left(\frac{m_a^A P_o K_a^2}{\sigma D_t^B u}\right) + C_3\left(\frac{D_o^2 P_o^{3/2} K_w^2}{\sigma D_t^B u}\right)\left(\frac{m_a^A P_o K_a^2}{\sigma D_t^B u}\right) + C_o \qquad (5.8)$$

where

C_n, C_a, A, B are regression coefficients

$$K_w = \frac{1}{1 + \frac{m_a}{2107.4 D_o^2 P_o^{1/2}}}$$

$$K_a = \frac{1}{1 + \frac{C_a m_a}{2107.4 D_o^2 P_o^{1/2}}}$$

corre-coef	P_o	D_o	D_t	m_a	u
P_o	1				
D_o	0.332	1			
D_t	0.134	0.274	1		
m_a	0.072	0.24	0.151	1	
u	-0.163	-0.268	-0.181	-0.107	1
H	0.618	0.559	-0.024	0.3	-0.315
W_t	0.16	0.152	0.933	0.266	-0.201

Table 4 Correlation between Operating Parameters

No.	Equations	Multiple corre-coeff R^2
1	$H = C_1 H_w + C_2 H_a + C_o$	0.88861
2	$H = C_1 H_w + C_2 H_a + C_3 H_w H_a + C_o$	0.95365
3	$H = C_1 H_w + C_2 H_a + C_3 H_w H_a + C_4 H_w^2 H_a + C_o$	0.95581
4	$H = C_1 H_w + C_2 H_a + C_3 H_w H_a + C_5 H_w H_a^2 + C_o$	0.95450
5	$H = C_1 H_w + C_2 H_a + C_3 H_w H_a + C_4 H_w^2 H_a + C_5 H_w H_a^2 + C_o$	0.96009
6	$H = C_1 H_w + C_2 H_a + C_3 H_w H_a + C_4 H_w^2 H_a + C_5 H_w H_a^2 + C_6 H_w^2 H_a^2 + C_o$	0.96012

Table 5 Determination of the Form of Regression Model

5.4 A Regression Model

Once the form of the model is determined, a regression model is readily available, as long as a sufficient body of experiments data is provided.

5.4.1 Determination of D_t^B

Eq (5.8) is used to determine the B value according to the regression analysis between H and D_t instead of between W_t and D_t. It will make the future model simpler. First we set: A=1, $\frac{2107.4}{C_a} = 550$ ($C_a = 3.832$). The result for eq(5.8) is demonstrated in table 6. Upon comparing the correlation coefficient R^2, we select B=0.85 as a value for the fitted model because of the highest correlation coefficient

B	1	0.9	0.85	0.8	0.7
R^2	0.9537	0.9588	0.9597	0.9594	0.9549

Table 6. Determination of D_t^B

5.4.2 Determination of A and C_a

As mentioned above, three criteria are employed to assess the quality of the regression analysis:

(1) multiple correlation coefficient R^2

(2) standard residual g_i

(3) the number of $g_i \leq \pm 2$

Table 7 shows the correlation coefficient R^2 for different combinations of A and C_a. Table 8 shows the number of $g_i \leq \pm 2$ for corresponding combinations. Figure 16-27 show the plot of standard residual g_i versus depth of cut H for the corresponding combinations.

A / $2107.4/C_a$	0.970	0.965	0.960
475	0.9602	0.9602	0.9602
500	0.9601	0.9601	0.9599
525	0.9599	0.9596	0.9594
550	0.9594	0.9591	0.9586

Table 7 Correlation Coefficient for Different Combinations of A And C_a (steel, 80 mesh, 150 data)

A / $2107.4/C_a$	0.970	0.965	0.960
475	7	5	5
500	5	5	6
525	5	6	5
550	5	5	5

Table 8 The Number of $g_i > \pm 2$ for Different Combinations of A and C_a (Steel, 80 mesh, 150 data)

After comparing the results of regression analysis at the different combinations of A and C_a. C_a=4.215 and A = 0.965 are selected because of the least number of $g_i > \pm 2$, the most even distribution and sufficiently high correlation coefficient. Finally, a regression model is determined as follows

$$H = C_1\left(\frac{D_o^2 P_o^{3/2} K_w^2}{\sigma D_t^{0.85} u}\right) + C_2\left(\frac{m_a^{0.965} P_o K_a^2}{\sigma D_t^{0.85} u}\right) + C_3\left(\frac{D_o^2 P_o^{3/2} K_w^2}{\sigma D_t^{0.85} u}\right)\left(\frac{m_a^{0.965} P_o K_a^2}{\sigma D_t^{0.85} u}\right) + C_o \qquad (5.9)$$

where

$$K_w = \frac{1}{1 + \frac{m_a}{2107.4 D_o^2 P_o^{1/2}}}$$

$$K_a = \frac{1}{1 + \frac{C_a m_a}{2107.4 D_o^2 P_o^{1/2}}}$$

CHAPTER 6

RESULTS AND DISCUSSIONS

In this chapter eq (5.9) is used to predict the depth of three various metals at different operational conditions. The accuracy of the prediction is made and then some inferences will be discussed.

6.1 Regression Results for the Regression Model (5.9)

Results of regression analysis of cutting of ductile materials are shown in Table 9 where the experimental data are taken from Databases 1,2,3,4 and 5. As it follows from this table all correlation coefficients are over 0.94. The fitted results which is the plot of fitted depth $\hat{H}$ versus observed depth H are depicted in Fig 28-33 for steel, aluminum and titanium, respectively. It shows that the regression fitting is so successful that at least 97% predicted data are located within the lines $\hat{H} = H \pm 2.5\text{mm}$ and at least 92% data are the region $H = H \pm 2(\text{mm})$.

Material	Abrasive size(mesh) No.of data	No. of data	C_a	C_o	C_1	C_2	C_3	R^2
Steel AISI 1018	50	38	5.520	-1.815	12.862	3.020	-5.819	0.9706
	80	150	4.215	-2.106	29.000	3.008	-7.701	0.9601
	220	24	1.054	-2.992	0.862	1.236	-0.558	0.9458
Aluminum	80	18	4.215	-1.787	66.718	4.817	-7.926	0.9939
Titanium	80	26	4.215	-1.091	32.335	2.834	-8.333	0.9831

Table 9 Results of Regression Analysis for All Materials

6.2 The Practical Meaning for Every Term in the Regression Model

From the model derivation, it follows that:

(1) $H_w = C_1 \frac{D_o^2 P_o^{3/2} K_w^2}{\sigma D_t^{0.85} u}$ represents the depth cut by water action,

(2) $H_a = C_2 \frac{m_a^{0.965} P_o K_a^2}{\sigma D_t^{0.85} u}$ represents the depth cut by abrasive action,

(3) $H_I = C_3 \left(\frac{D_o^2 P_o^{3/2} K_w^2}{\sigma D_t^{0.85} u} \right) \left(\frac{m_a^{0.965} P_o K_a^2}{\sigma D_t^{0.85} u} \right)$ represents the depth caused by the interaction between water and abrasive particle. C_3 is always negative. It means that the interaction between water and particle would be intervened each other and would reduce the total depth of cut during the cutting.

(4) C_0 represents the energy loss due to friction and collision existing among water, particle and tube wall. Negative sign shows that energy loss in the course of cutting exists.

Database 6 demonstrates the changes of H_w, H_a, H_I and $\hat{H}$ along with the change of operating parameters during cutting steel with the abrasive size 80 mesh.

6.3 Correlation of Depth of Cut and Operating Parameters

It is interesting to show that patterns of the relationship between H_W , H_a and process variables are similar. Comparative effect of various parameters on cutting results are shown in table 10. The first column contains the correlation coefficients between H_W and operating parameters. It has been found that sapphire diameter D_O has the largest effect on H_W. Water pressure P_O lies the next. There no effect of m_a on H_W (correlation coefficient is 0.062). This proves that H_W represents a pure water action. In the H_a column, similar effects of the parameters happened to H_a. Correlation coefficient between H and the process parameters shows that D_o and P_O has the main effects on H, while the effect of m_a

is secondary. The effect of D_t and u is negative on the depth of cut, but the correlation coefficient between D_t and H is low and goes beyond the cutting experience.

Depth(mm) / Parameters	H_w	H_a	H
P_0 (MPa)	0.459	0.535	0.622
D_0 (mm)	0.794	0.627	0.574
D_t (mm)	-0.009	-0.069	-0.027
m_a (g/min)	0.062	0.277	0.326
u (cm/min)	-0.115	-0.213	-0.145

Table 10 Correlation between Depth and Operating Parameters
(Steel AISI 1018, 80 mesh Abrasive)

6.4 Effects of Water and Abrasive on the Depth of Cut

The previous works did not separate effects of water and particles on the depth of cut. In the most studies the water action was ignored. Water was considered as energy transfer media. In this study, an important inference was drawn from the model (5.9). If we consider water effect and abrasive effect on depth of cut separately, the model (5.9) will become:

$$H = C_1 H_w + C_2 H_a \tag{6.1}$$

We can evaluate the percentage of water action and percentage of abrasive action, respectively as follows:

$$P_w = \frac{C_1 H_w}{C_1 H_w + C_2 H_a} \times 100\% \qquad \text{(for water action)} \tag{6.2}$$

$$P_a = \frac{C_1 H_a}{C_1 H_w + C_2 H_a} \times 100\% \qquad \text{(for abrasive action)} \tag{6.3}$$

The results of the computation of percentages of each action (steel, 80 mesh) are listed in Database 6, which shows that water contribution can reach 10% of the total result. If we deleted the water action (C_1H_W) term and use the abrasive action term only, the correlation coefficient becomes R=0.93. The consideration of water action increases correlation coefficient from 0.93 to 0.96.

6.5 Prediction of the Water Velocity and the Abrasive Velocity at the Exit of Tube

Another inference which can be drawn from the model (5.9) is the prediction of the water velocity and the abrasive velocity at the exit of carbide nozzle. In chapter 5 we derived the velocity equations as follows:

$$V_{sw} = \sqrt{\frac{2P_o}{\rho_w}} = \sqrt{2000}\, P_o^{1/2} \tag{6.4}$$

$$V_{cw} = \frac{1}{1 + \frac{m_a}{2107.4\, D_o^2 P_o^{1/2}}} V_{sw} \tag{6.5}$$

$$V_a = \frac{1}{1 + \frac{C_a m_a}{2107.4\, D_o^2 P_o^{1/2}}} V_{sw} \tag{6.6}$$

where

$C_a = 5.520$ for 50 mesh

$C_a = 4.215$ for 80 mesh

$C_a = 1.054$ for 220 mesh

In the above equations, V_{sw} is the theoretical water velocity at the exit of the sapphire obtained from the Bernoulli's equation. V_{cw} is the water velocity at the exit of carbide tube. V_a is the abrasive particles velocity at the exit of carbide tube. Because C_a value is received from regression analysis for the depth of cut, it follows that V_a is derived from the actual depth of cut. The derived results for three different sizes of particle are listed in the Database 7, 8 and 9 and depicted in the Figure 34-39.

Figure 34 shows the plot of Bernoulli's equation. The water velocity from sapphire Vsw is determined by pressure P_o. Figure 35-37 show the relationship of m_a versus V_a and m_a versus V_{cw}. It is showed that when m_a increases, V_a and V_{cw} decrease. The Figure 38 and 39 show the relationship between V_a and operating parameters. When m_a is over 300 g/min, the curve becomes flat and V_a does not decrease. That is suggested that the equation (6.6) is suitable for $m_a < 300$ g/min.

6.6 Relationship Between Particle Coefficient C_a and the Size of Particle

It was assumed that C_a accounts for the effects of particle size and collision among water, abrasive and tube wall on the V_a. When the size of particle increase, C_a increases. A chart (Fig 40) and Table 11 show the correlation between C_a and particle size.

Size of particle (mesh)	Diameter of particle (μm)	C_a
50	300	5.520
80	177	4.215
220	65	1.054

Table 11 C_a Values for Different Sizes of the Particle

CHAPTER 7

CONCLUSIONS AND RECOMMENDATIONS

7.1 Conclusions

(1) The semi-empirical equation (5.9) is an effective model describing the relationship between depth of cut and cutting parameters, while statistical analysis enables us to examine some phenomena which occur in the course of AWJ cutting and were not examined in the published reports.

(2) The prediction technique developed in this study can be used in the industrial condition because it included readily available information about operating conditions and material properties.

(3) A developed model includes water action, particle action and interaction between the water and particle. The cutting results can be predicted with correlation coefficient of over 0.94 for three different ductile materials and three kinds of particle sizes. We also can predict the contribution of water action and particle action at different combinations of operating parameters. It has been found that the contribution of water action is under 10% within the normal range of operating parameters.

(4) For the existing range of the process parameters water pressure P_0 and sapphire diameter D_0 have the strongest correlation with cutting depth. The effect of m_a is weaker, while the effect of other parameters is practically negligible.

(5) The velocities of water and abrasive particle at the exit of nozzle can be evaluated through macroscopic statistical analysis. Three theoretical equations for the velocities are suggested to show how the velocities are distributed at the exit of nozzle.

7.2 Recommendations

To get a complete prediction model for the machining results in the AWJ machining, it is necessary:

(1) to do more experiments for other materials including ductile and brittle materials to see the practicability of the prediction model.

(2) to investigate the effect of the nozzle design on the applications of the prediction model.

(3) to improve information concerning particles velocity distribution.

(4) to investigate cutting of the workpiece thickness exceeding 2 inches.

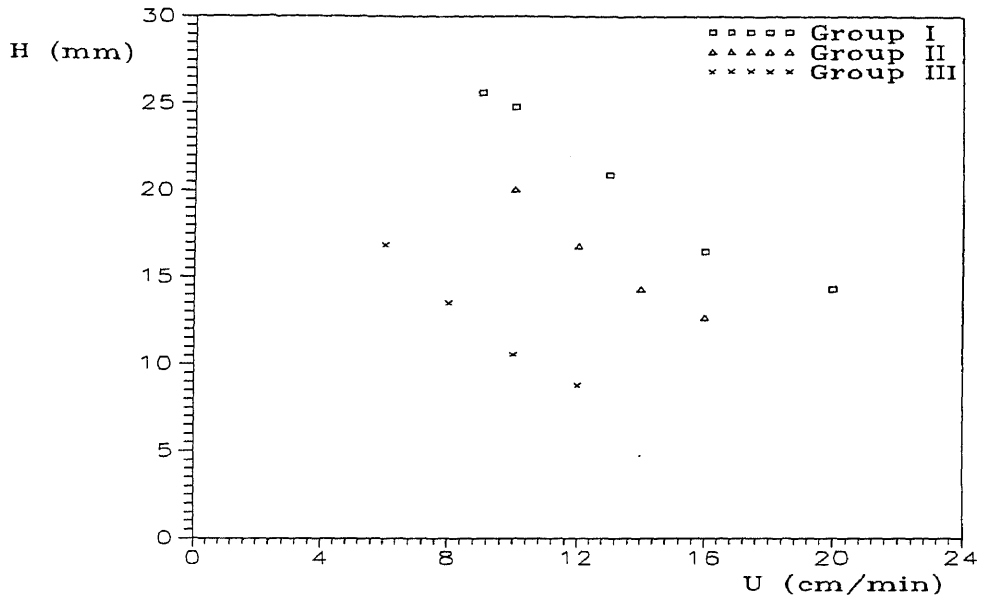

Figure 12 Effect of Traverse Speed on the Depth of Cut
(Steel AISI 1018, P_o=317MPa; S_a =177μm; Group I: D_o=0.305mm, D_t=0.838mm, M_a=275g/min; Group II: D_o=0.152mm, D_t=0.838mm, M_a=204g/min; Group III: D_o=0.254mm, D_t=1.195mm, M_a=209g/min)

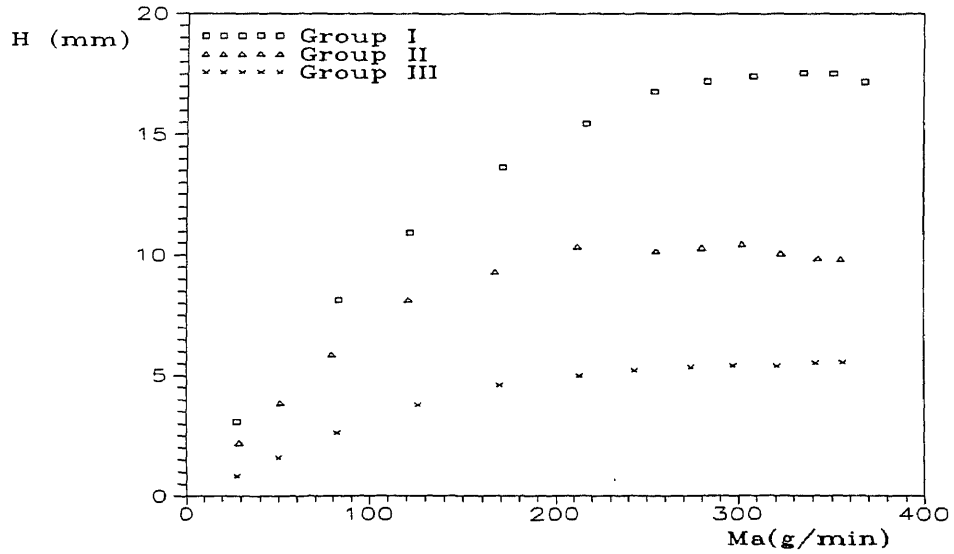

Figure 13 Effect of Abrasive Mass Flow Rate on Depth of Cut
(Steel AISI 1018, S_a =177μm; Group I: P_o=317MPa; D_o=0.254mm, D_t=0.865mm, U=14cm/min; Group II: P_o=317MPa; D_o=0.177mm, D_t=0.906mm, U=14cm/min; Group III: P_o=331MPa; D_o=0.177mm, D_t=1.015mm, U=10cm/min)

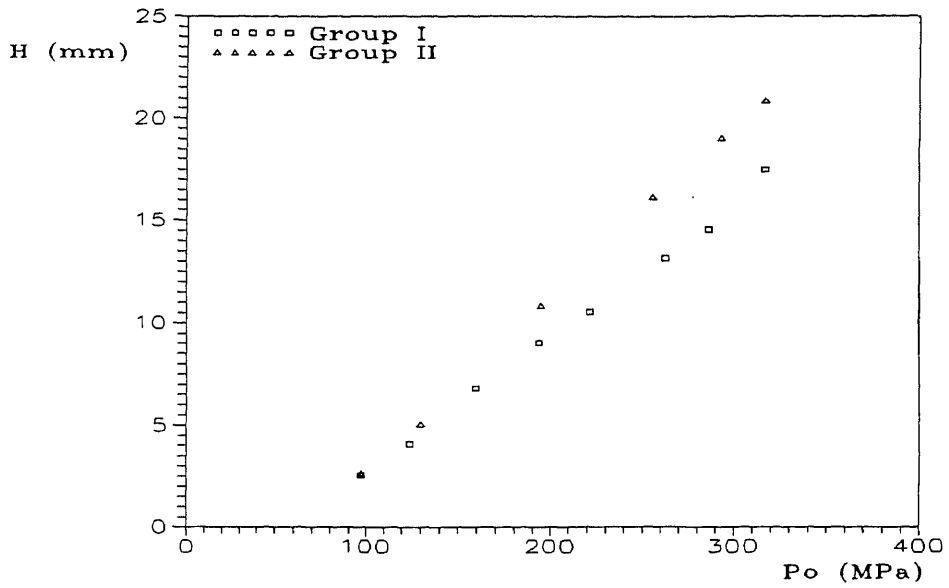

Figure 14 Effect of Abrasive Mass Flow Rate on Depth of Cut
(Steel AISI 1018, S_a = 177μm; D_o=0.254mm, U=12cm/min;
Group I: D_t=1.092mm, M_a=242g/min;
Group II: D_t=0.838mm, M_a=303g/min)

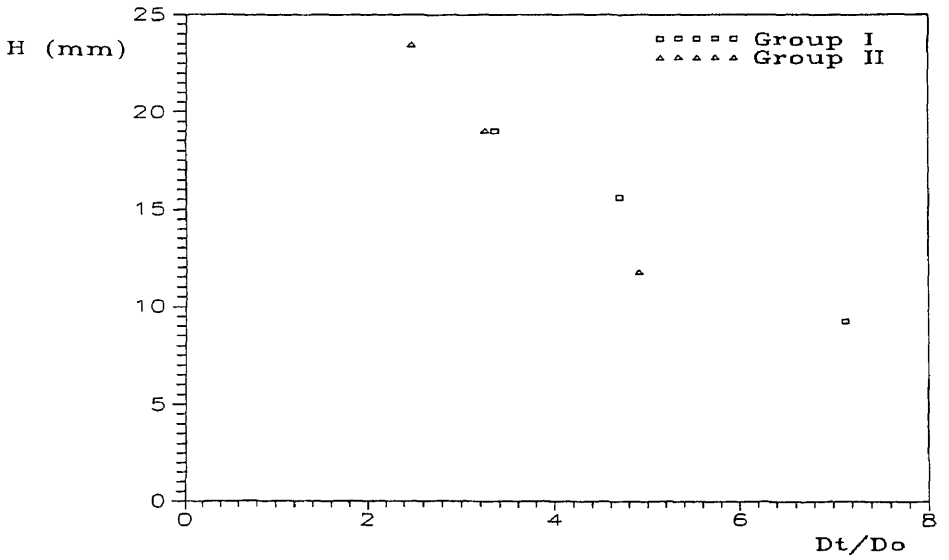

Figure 15 Effect of Nozzle Combination on Depth of Cut
(Steel AISI 1018, P_o=317MPa; S_a = 177μm; Group I:
D_o=0.254mm, M_a=260g/min;U=14cm/min; Group II:
D_o=0.365mm, M_a=280g/min; U=13cm/min)

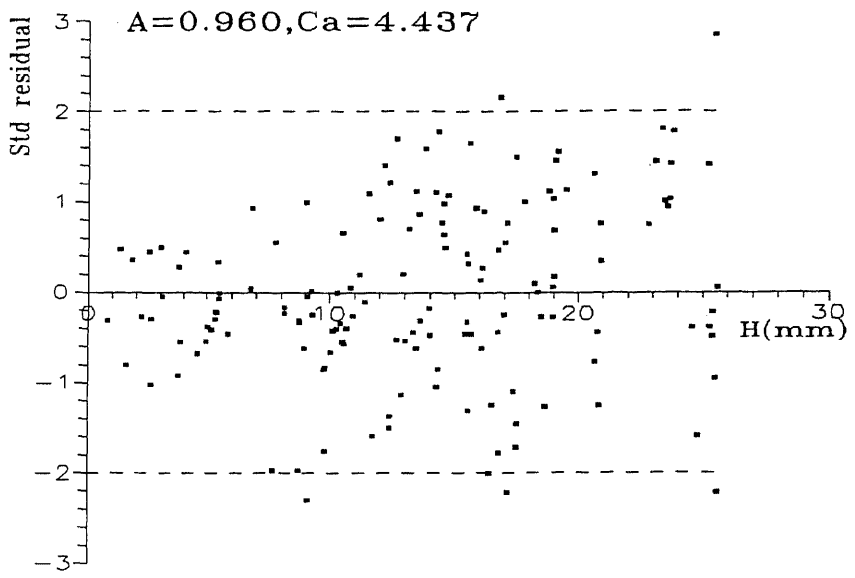

Figure 16 Plot of Standard Residual g_i versus Depth of Cut H
(A=0.960, C_a=4.437)

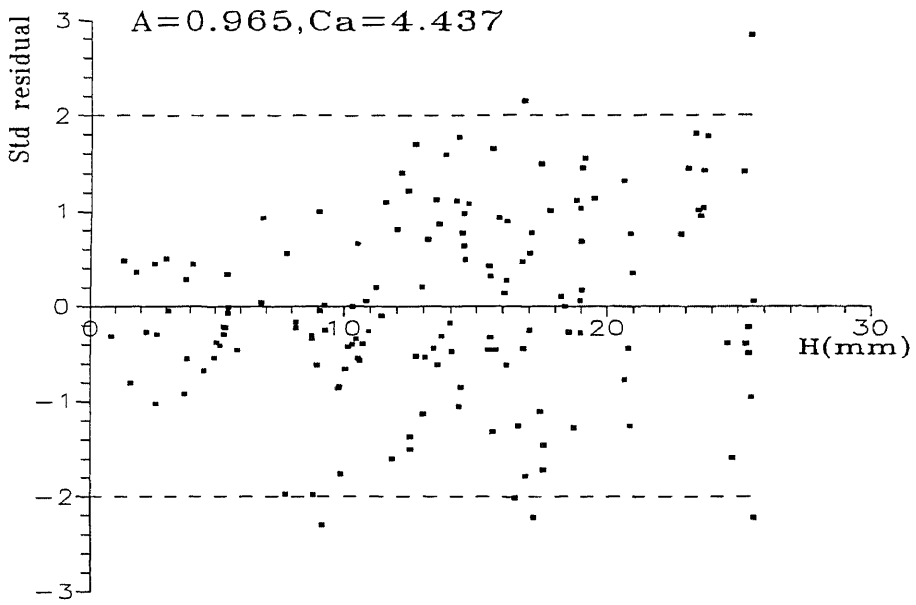

Figure 17 Plot of Standard Residual g_i versus Depth of Cut H
(A=0.965, C_a=4.437)

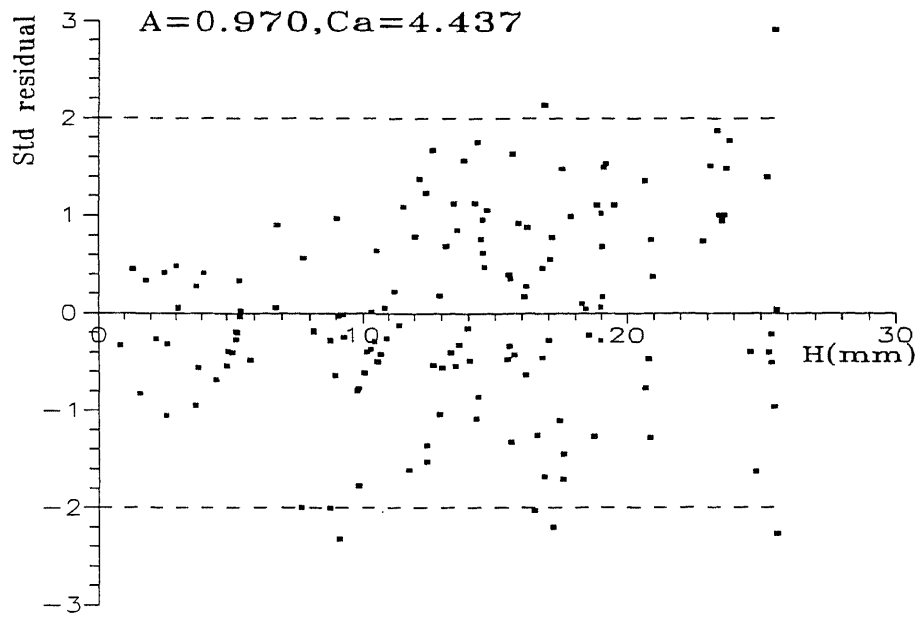

Figure 18 Plot of Standard Residual g_i versus Depth of Cut H
(A=0.970, C_a=4.437)

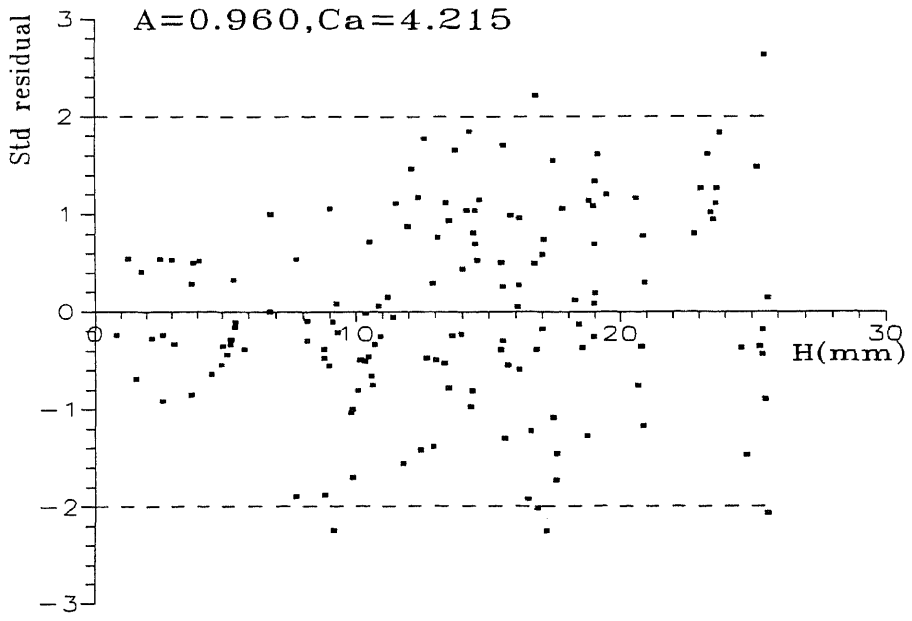

Figure 19 Plot of Standard Residual g_i versus Depth of Cut H
(A=0.960, C_a=4.215)

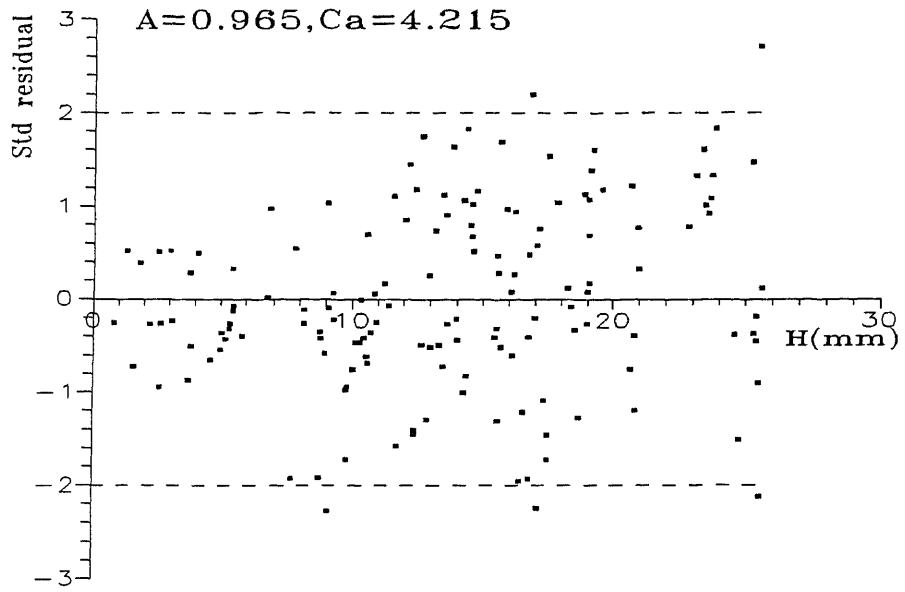

Figure 20 Plot of Standard Residual g_i versus Depth of Cut H
(A=0.965, C_a=4.215)

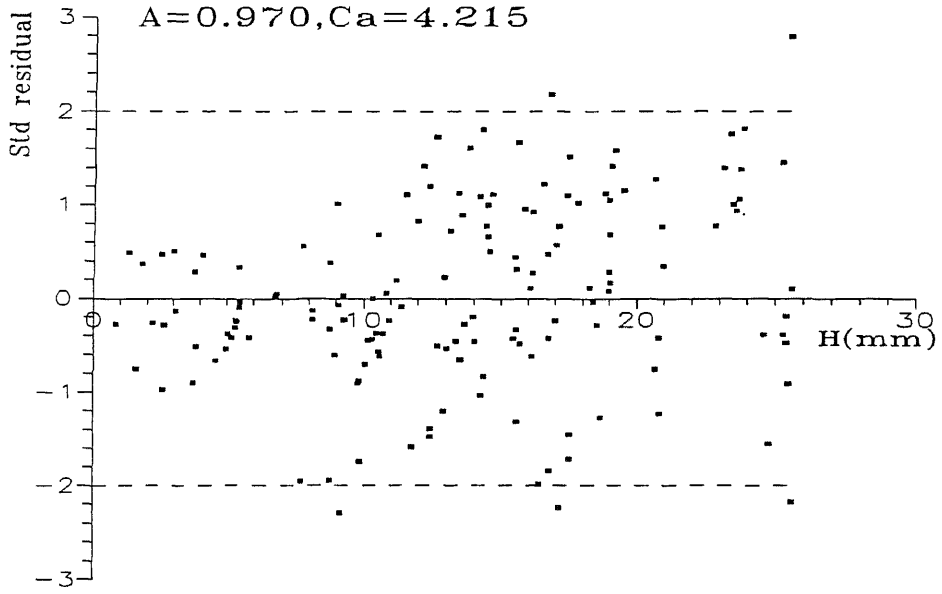

Figure 21 Plot of Standard Residual g_i versus Depth of Cut H
(A=0.970, C_a=4.215)

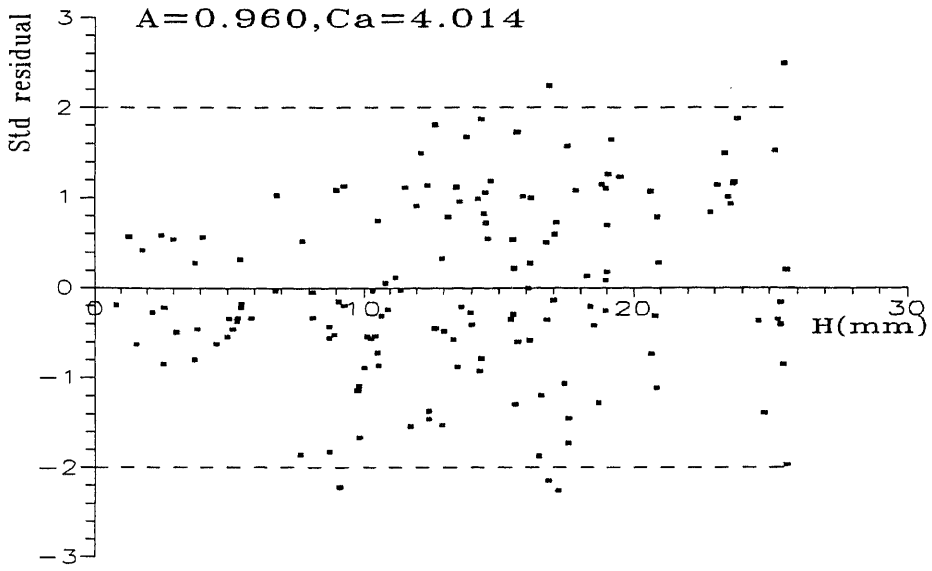

Figure 22 Plot of Standard Residual g_i versus Depth of Cut H
(A=0.960, C_a=4.014)

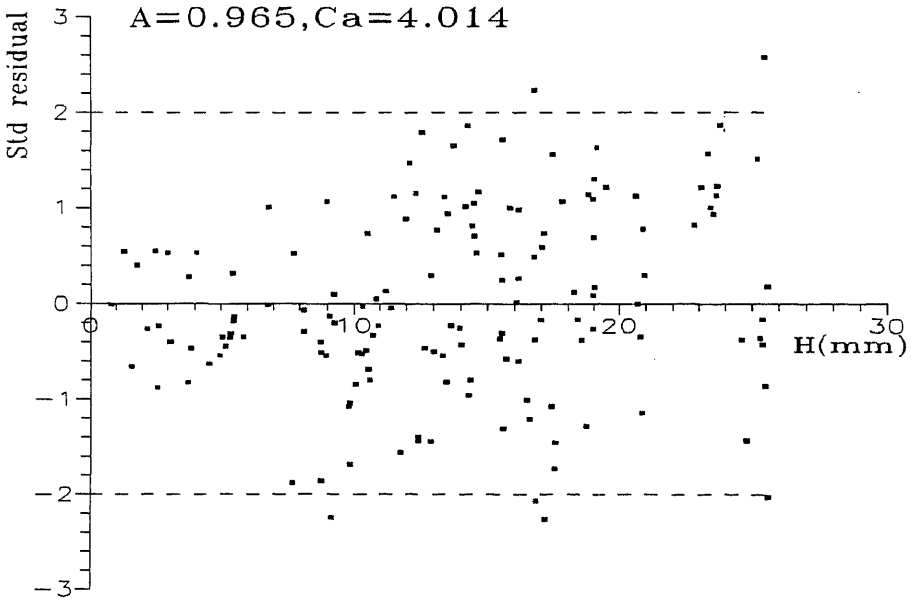

Figure 23 Plot of Standard Residual g_i versus Depth of Cut H
(A=0.965, C_a=4.014)

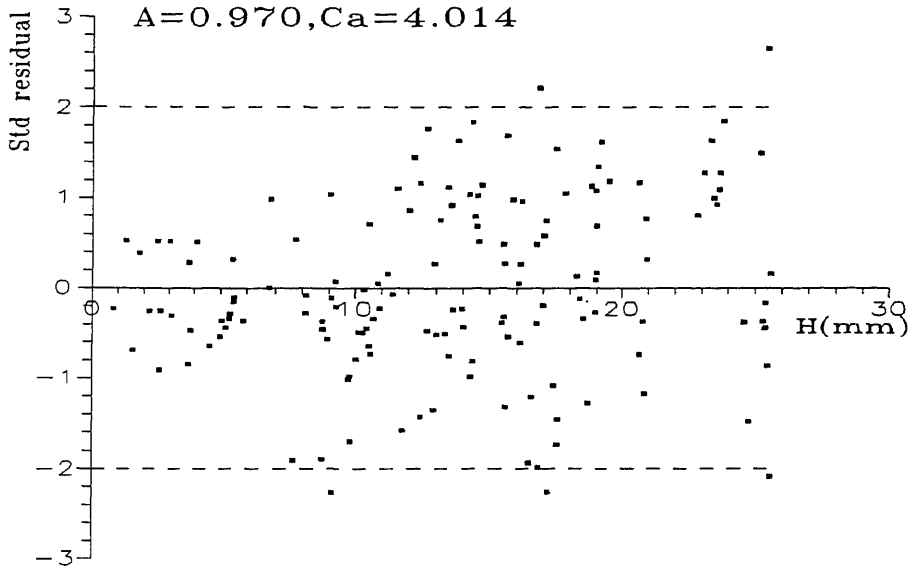

Figure 24 Plot of Standard Residual g_i versus Depth of Cut H
(A=0.970, C_a=4.014)

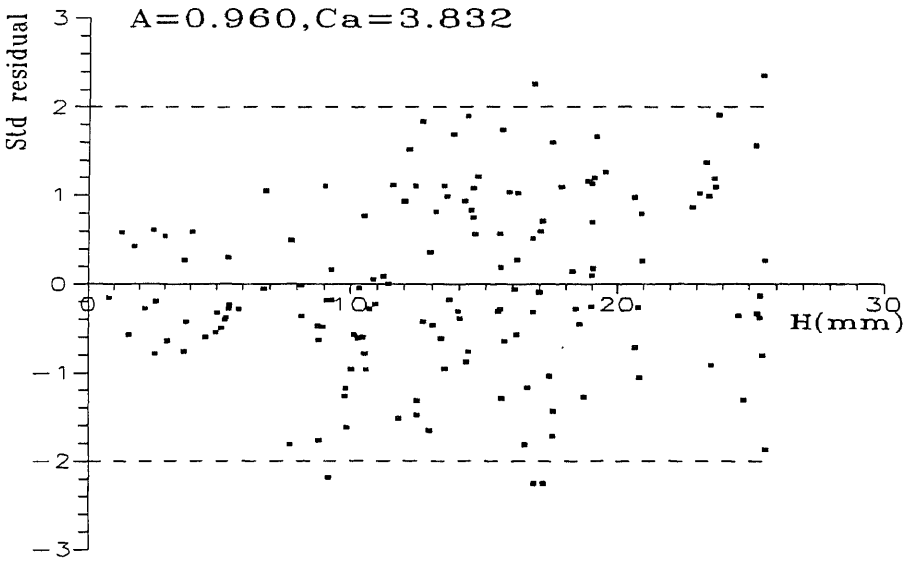

Figure 25 Plot of Standard Residual g_i versus Depth of Cut H
(A=0.960, C_a=3.832)

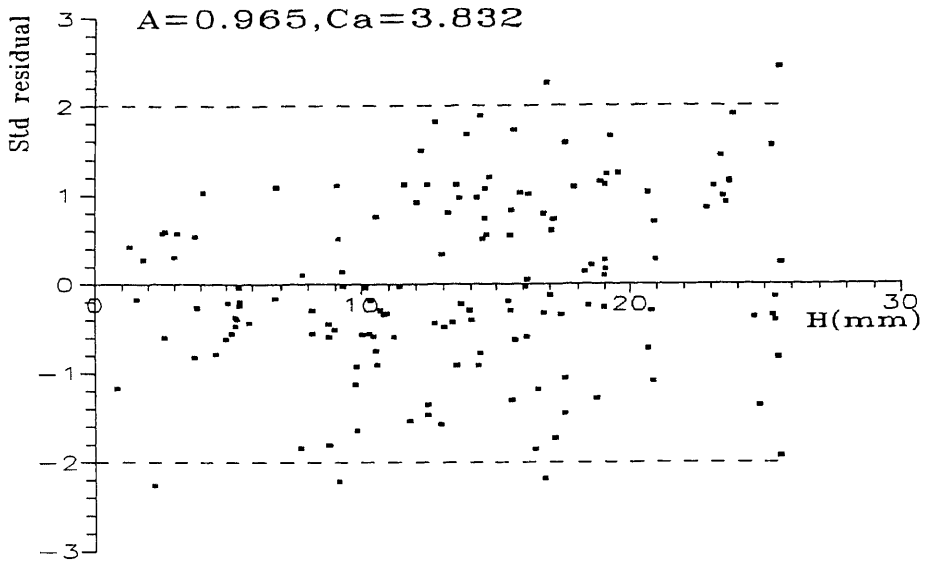

Figure 26 Plot of Standard Residual g_i versus Depth of Cut H
(A=0.965, C_a=3.832)

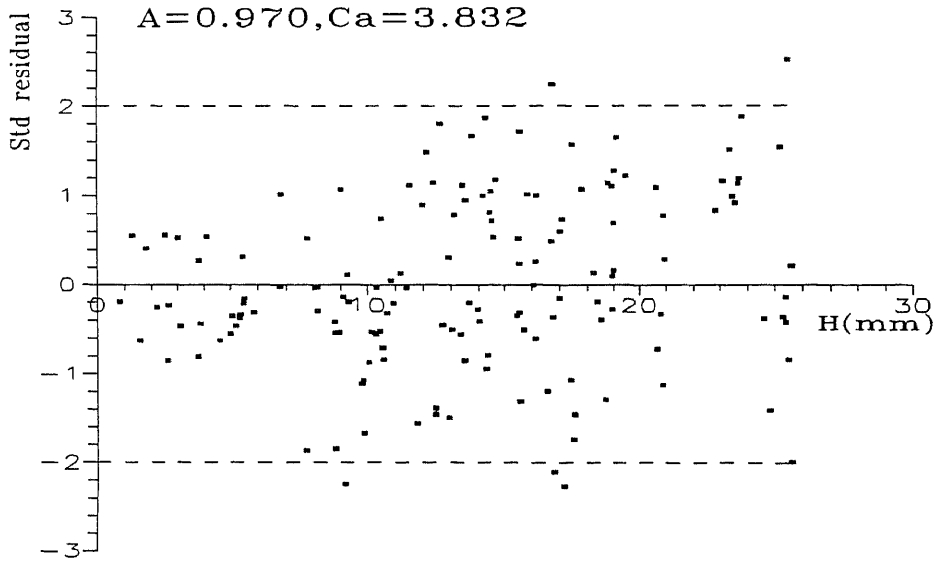

Figure 27 Plot of Standard Residual g_i versus Depth of Cut H
(A=0.970, C_a=3.832)

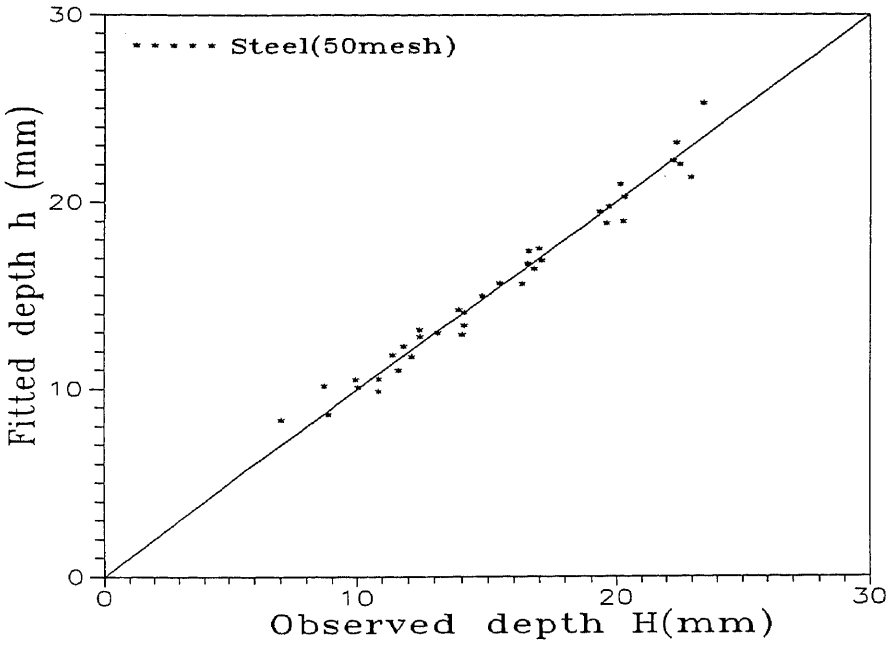

Figure 28 Plot of Fitted Depth $\hat{H}$ versus Observed Depth of Cut
(Steel AISI 1018, Size of Abrasive = 50 Mesh)

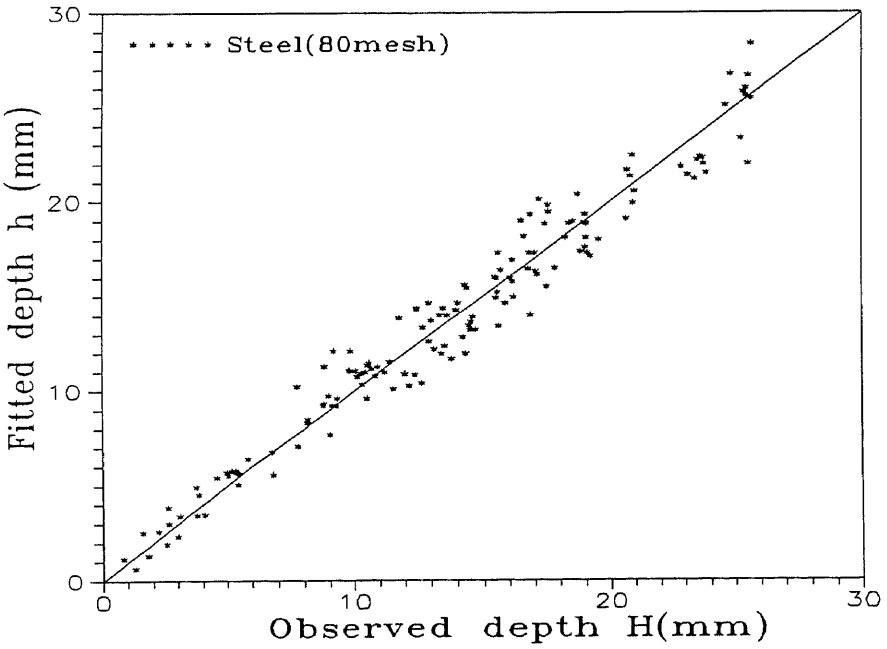

Figure 29 Plot of Fitted Depth $\hat{H}$ versus Observed Depth of Cut H
(Steel AISI 1018, Size of Abrasive = 80 Mesh)

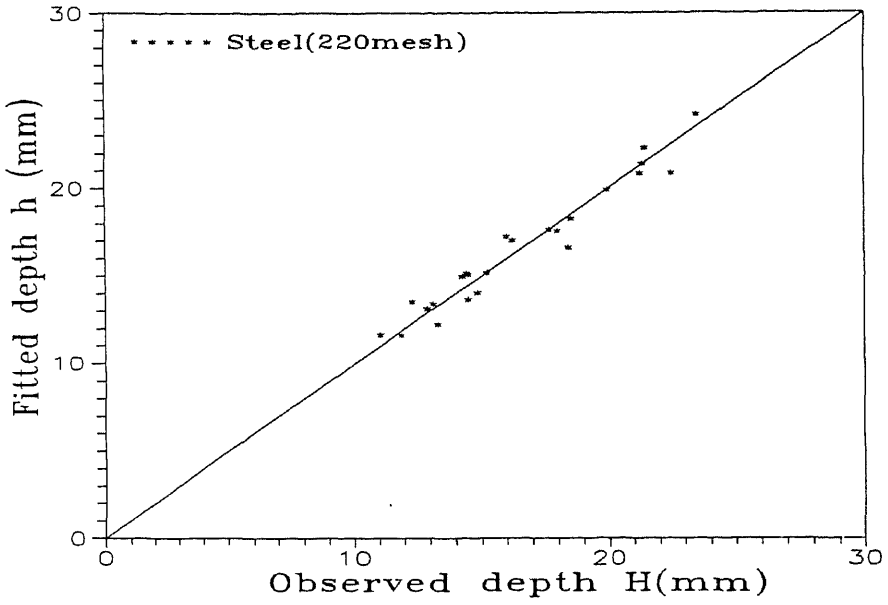

Figure 30 Plot of Fitted Depth $\hat{H}$ versus Observed Depth of Cut H
(Steel AISI 1018, Size of Abrasive = 220 Mesh)

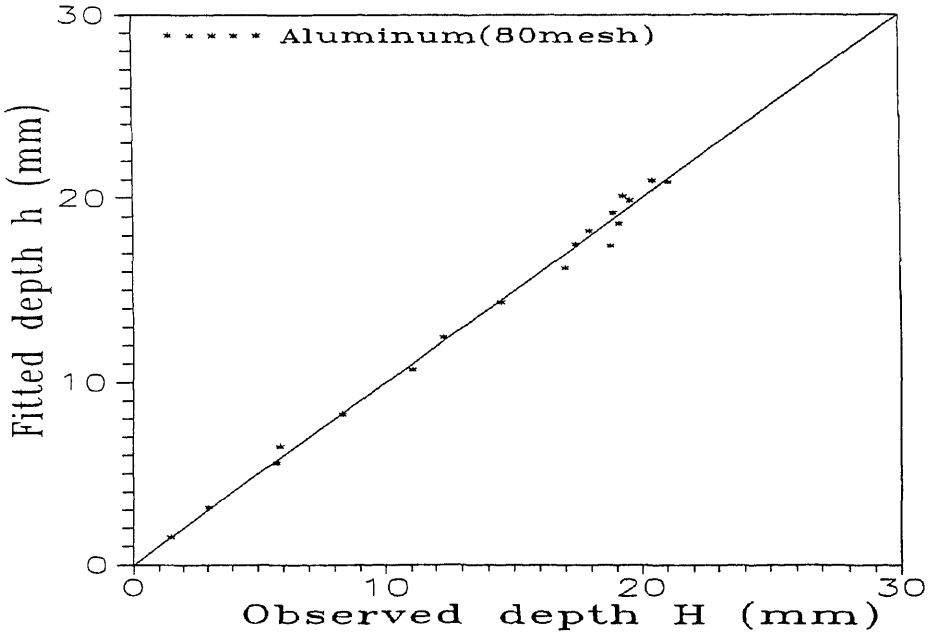

Figure 31 Plot of Fitted Depth $\hat{H}$ versus Observed Depth of Cut H
(Aluminum, Size of Abrasive = 80 Mesh)

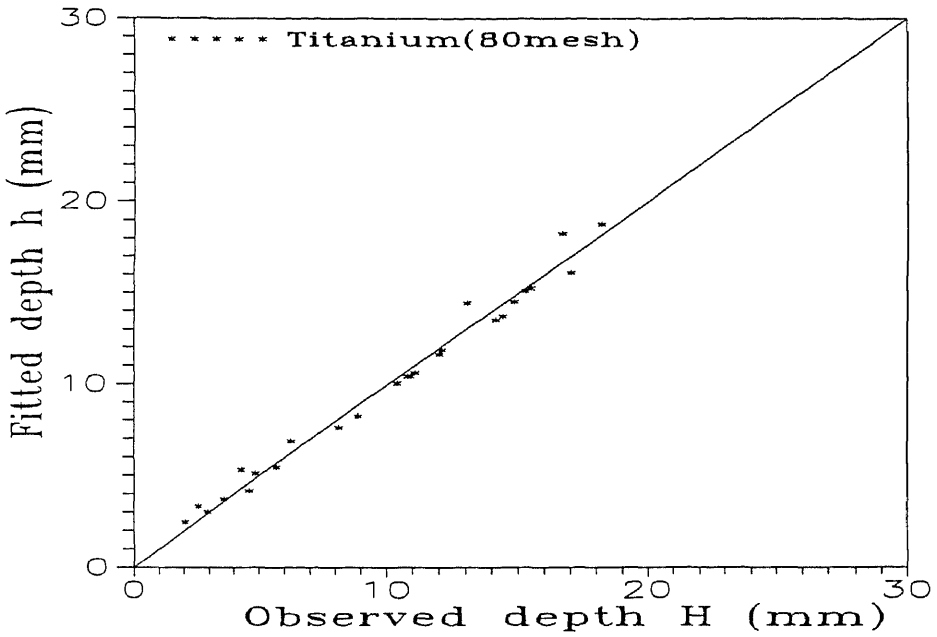

Figure 32 Plot of Fitted Depth $\hat{H}$ versus Observed Depth of Cut H
(Titanium, Size of Abrasive = 80 Mesh)

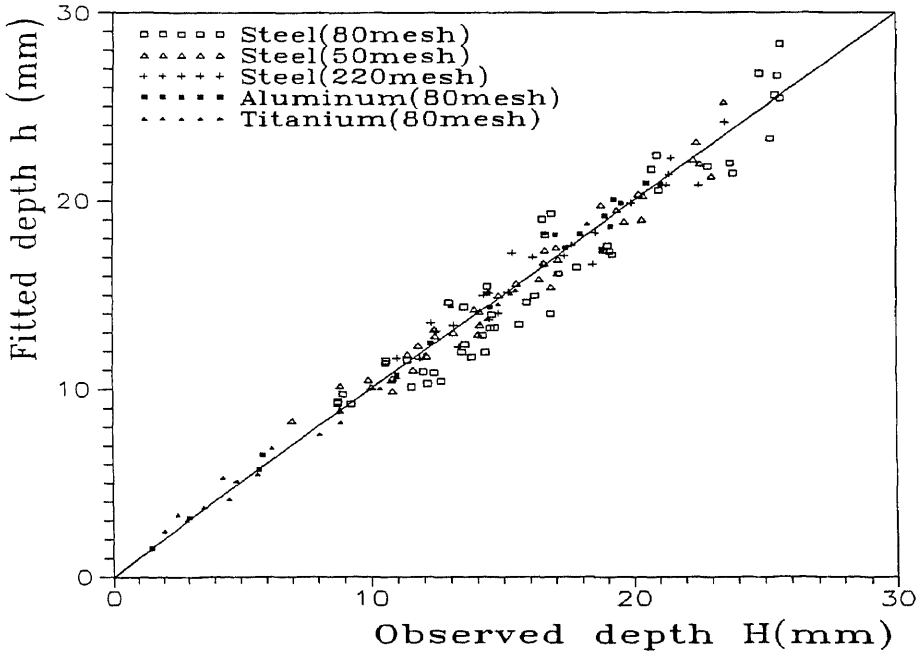

Figure 33 Plot of Fitted Depth $\hat{H}$ versus Observed Depth of Cut H
(All Materials and Size of Abrasive)

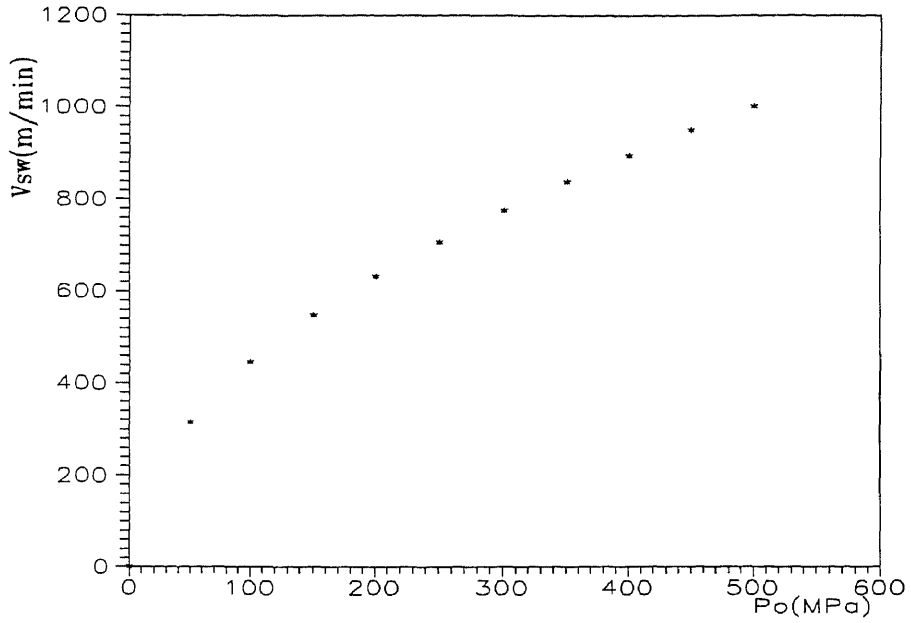

Figure 34 Water Velocity from Sapphire Nozzle
according to Bernoulli's Equation

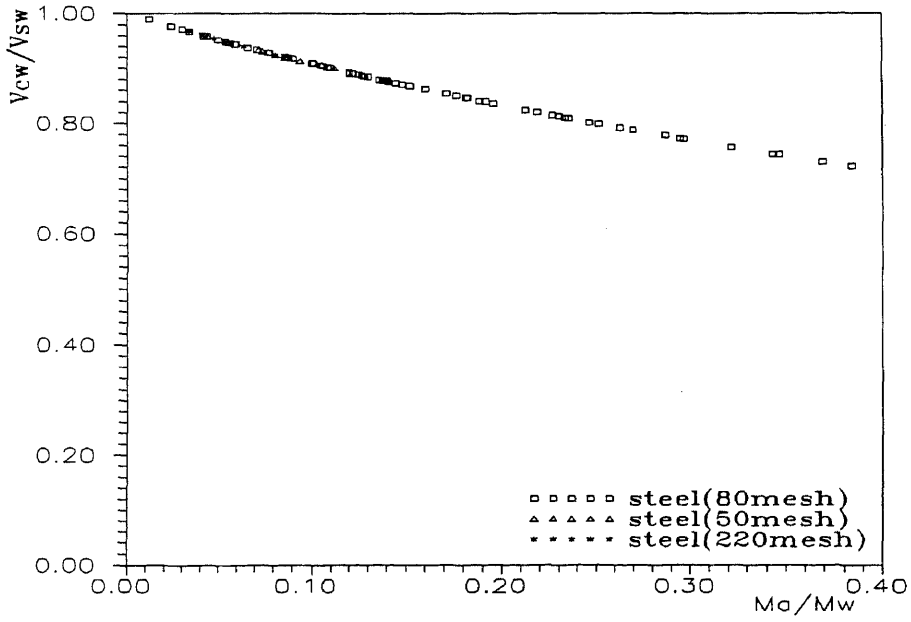

Figure 35 Predicted Water Velocity at the Exit of Carbide Tube
(Steel AISI 1018)

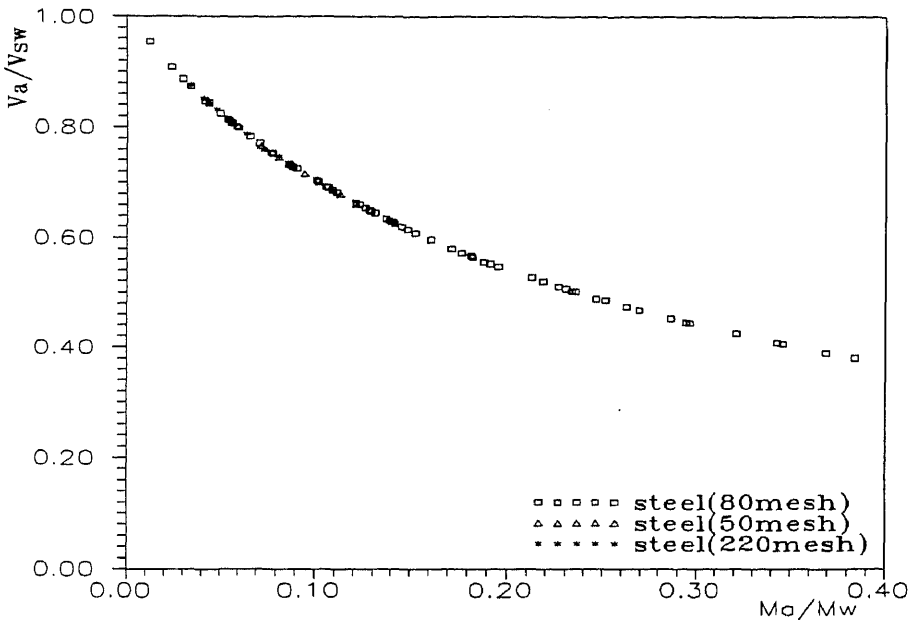

Figure 36 Abrasive Velocity at the Exit of Carbide Tube Associated with Water Velocity at the Exit of Sapphire Nozzle (Steel AISI 1018)

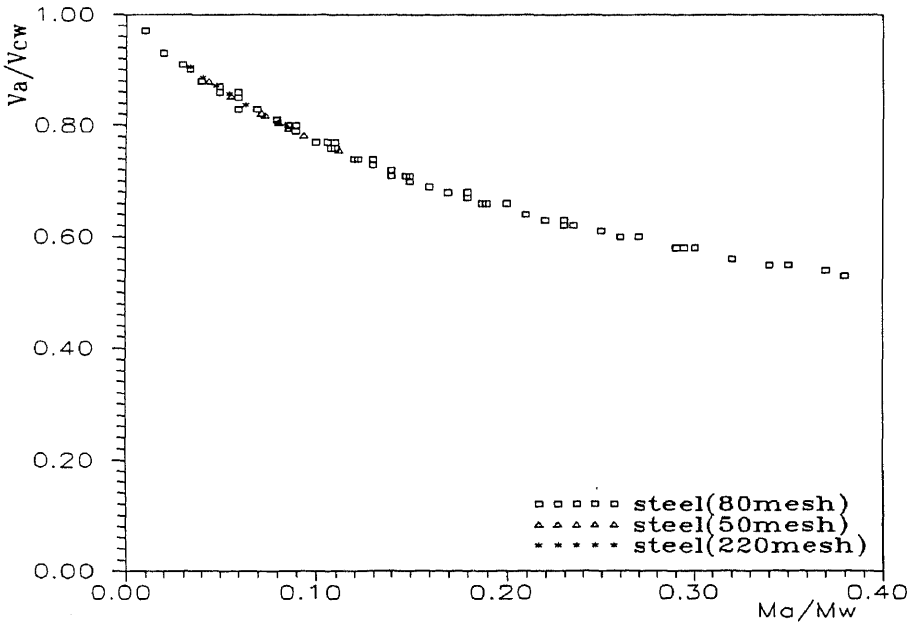

Figure 37 Abrasive Velocity at the Exit of Carbide Tube Associated with Water Velocity at the Exit of Carbide Tube (Steel AISI 1018)

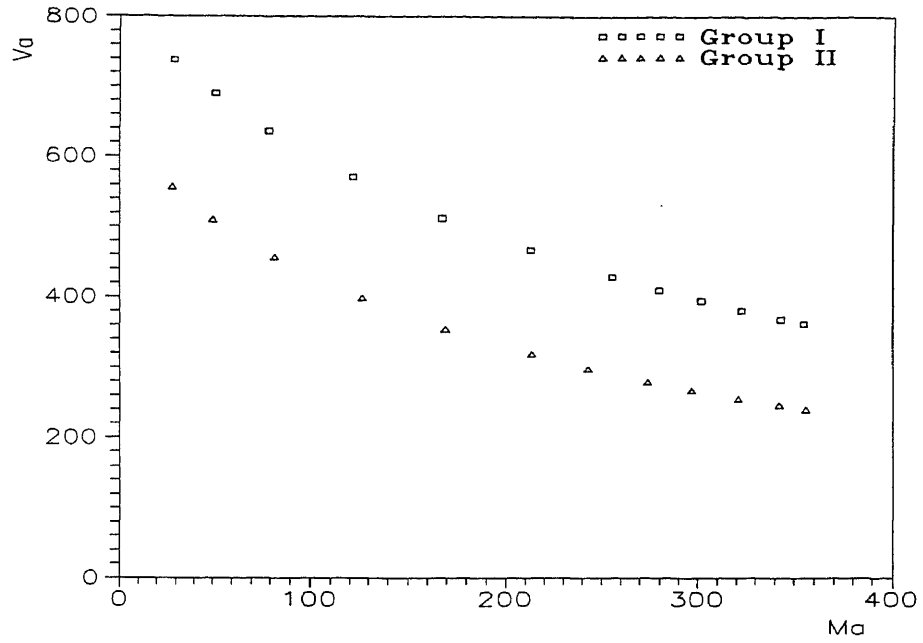

Figure 38 Relationship I between V_a and Operating Parameters (Steel, 80mesh, D_0=0.177mm,Group I: P_0=331PMa, D_t=0.906mm, U=14g/min; Group II: P_0=197PMa, D_t=1.01mm, U=10g/min;)

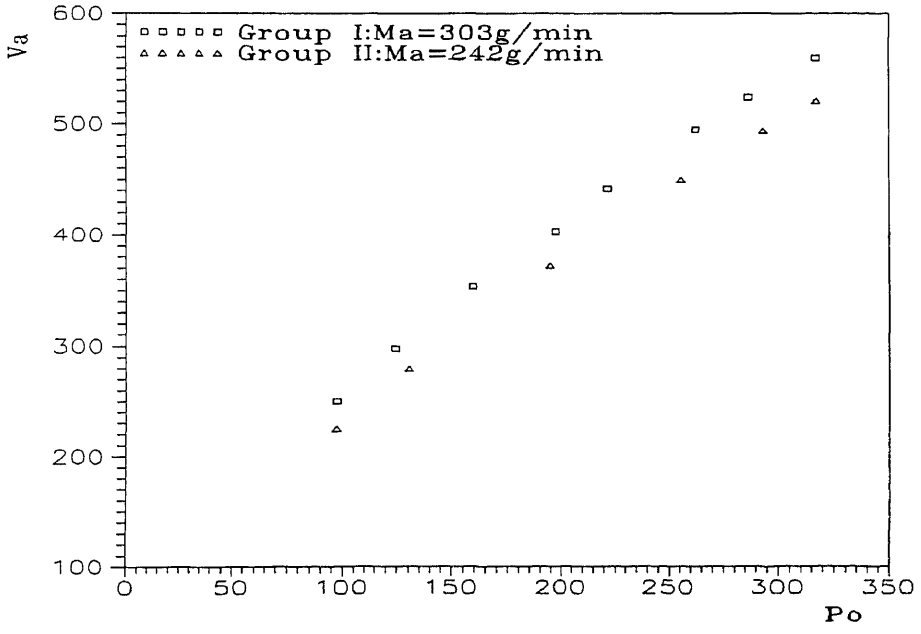

Figure 39 Relationship II between V_a and Operating Parameters (Steel, 80mesh, D_0=0.254mm, U=12cm/mim;Group I: Ma=303g/min, D_t=1.155mm; Group II: Ma=242g/min, D_t=0.916mm)

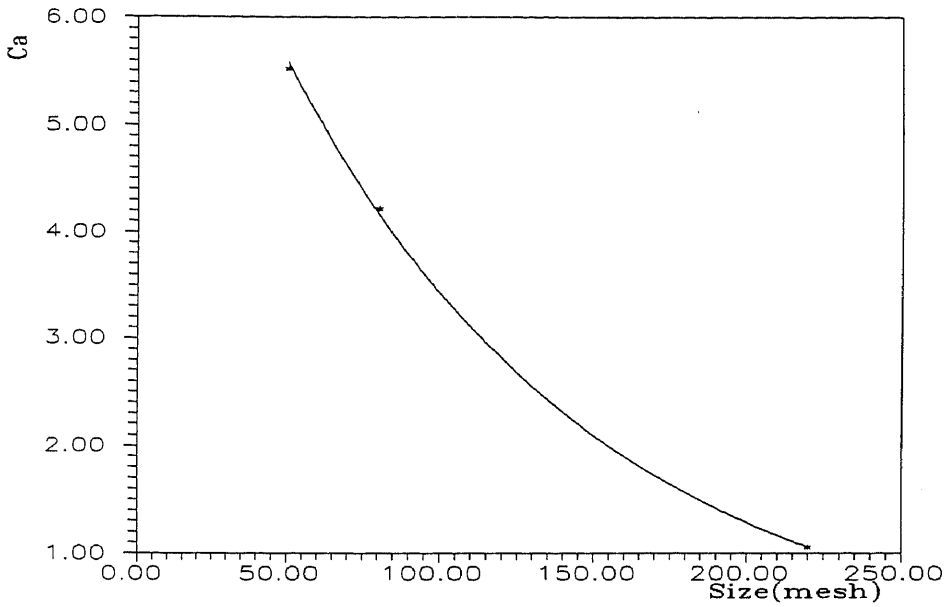

Figure 40 Plot of the Relationship between C_a and the Size of Abrasive

APPENDIX

DATABASE OF EXPERIMENTAL AND CALCULATED RESULTS

This appendix includes the following defined letters:

P_i	Initial water pressure (MPa)
P_o	Operating water pressure (MPa)
D_o	Diameter of sapphire orifice (mm)
D_t	Diameter of carbide tube (mm)
M_a	Mass flow rate of abrasive (g/min)
M_w	Mass flow rate of water (g/min)
S_a	Size of abrasive (mesh)
S_d	Standoff distance (mm)
U	Traverse speed of the nozzle (cm/min)
W_t	Top kerf width (mm)
H_w	Fitted depth of cut caused by water action (mm)
H_a	Fitted depth of cut caused by abrasive action (mm)
H_I	Fitted depth of cut caused by the interaction between water and abrasive(mm)
H	Total observed depth of cut by AWJ (mm)
$\hat{H}$	Total fitted depth of cut (mm)
C_1, C_2, C_3	Regression coefficient determined by regression analysis
P_W	Percentage of water action on the depth of cut (%)
Pa	Percentage of abrasive action on the depth of cut (%)
V_{SW}	Water velocity at the exit of sapphire nozzle (m/min)
Vcw	Water velocity at the exit of carbide nozzle (m/min)
Va	Abrasive particle velocity at the exit of carbide nozzle (m/min)

Database 1

(Use Water Nozzles and Nozzle Body of New Design)
Steel AISI 1018, S_a=80 mesh (Barton's HPE), S_d=2.5 mm

No.	Po(MPa)	Do(mm)	Dt(mm)	Ma(g/min)	U(cm/min)	Wt(mm)	H(mm)
001	317	0.152	0.838	204	6	1.328	16.83
002	317	0.152	0.838	204	8	1.224	13.50
003	317	0.152	0.838	204	10	1.446	10.55
004	317	0.152	0.838	204	12	1.334	8.77
005	317	0.152	0.838	255	8	1.288	12.94
006	317	0.152	0.838	255	10	1.238	10.59
007	317	0.152	0.838	255	12	1.269	8.78
008	317	0.203	1.118	229	7	1.524	20.94
009	317	0.203	1.118	229	9	1.474	17.10
010	317	0.203	1.118	229	12	1.480	13.43
011	317	0.203	1.118	229	14	1.464	11.55
012	317	0.203	1.118	229	7	1.516	23.70
013	317	0.203	1.118	229	9	1.503	19.05
014	317	0.203	1.118	229	12	1.514	14.21
015	317	0.203	1.118	229	14	1.520	12.39
016	317	0.203	0.851	211	8	1.072	25.60
017	317	0.254	0.851	211	9	1.297	25.22
018	317	0.254	0.851	211	10	1.204	23.82
019	317	0.254	0.851	211	13	1.134	19.16
020	317	0.254	0.851	211	15	1.156	16.17
021	317	0.254	0.851	211	17	1.176	14.68
022	317	0.254	0.851	256	11	1.251	22.83
023	317	0.254	0.851	256	14	1.185	18.97
024	317	0.254	0.851	256	17	1.218	15.85
025	317	0.254	0.851	256	20	1.190	13.55
026	317	0.254	1.195	209	12	1.490	16.80
027	317	0.254	1.195	209	14	1.495	14.31
028	317	0.254	1.195	209	16	1.491	12.65
029	317	0.254	1.195	262	16	1.475	13.79
030	317	0.254	1.195	262	14	1.544	15.60
031	317	0.254	1.195	262	18	1.522	12.16
032	317	0.254	1.810	262	12	2.127	12.00
033	317	0.254	1.810	262	10	2.203	14.51
034	317	0.254	1.810	262	8	2.242	17.80
035	317	0.254	1.810	262	14	2.249	9.27
036	317	0.254	1.810	295	18	2.163	18.80

No.	Po(MPa)	Do(mm)	Dt(mm)	Ma(g/min)	U(cm/min)	Wt(mm)	H(mm)
037	317	0.254	1.810	295	10	2.160	14.58
038	317	0.254	1.810	295	12	2.220	11.41
039	317	0.254	1.810	295	14	2.250	8.97
040	317	0.308	0.825	212	7	1.004	25.50
041	317	0.308	0.825	212	8	1.319	25.40
042	317	0.308	0.825	212	11	1.211	20.67
043	317	0.308	0.825	212	14	1.214	16.57
044	317	0.308	0.825	212	17	1.209	14.37
045	317	0.308	0.825	275	9	1.077	25.60
046	317	0.308	0.825	275	11	1.324	24.60
047	317	0.308	0.825	275	13	1.171	20.87
048	317	0.308	0.825	275	16	1.156	16.47
049	317	0.308	0.825	275	20	1.151	14.30
050	317	0.308	1.146	278	10	1.381	23.67
051	317	0.308	1.146	278	13	1.401	19.50
052	317	0.308	1.146	278	16	1.390	15.50
053	317	0.308	1.146	278	19	1.376	13.93
054	317	0.308	1.146	210	10	1.436	18.97
055	317	0.308	1.146	210	12	1.416	17.03
056	317	0.308	1.146	210	15	1.395	12.70
057	317	0.308	1.146	210	18	1.397	10.70
058	317	0.308	1.860	210	9	2.033	14.03
059	317	0.308	1.860	210	7	2.108	18.23
060	317	0.308	1.860	210	11	2.085	9.87
061	317	0.308	1.860	210	13	2.074	7.73
062	317	0.308	1.860	277	9	2.076	17.00
063	317	0.308	1.860	277	11	2.065	12.47
064	317	0.308	1.860	277	7	2.175	2.80
065	317	0.308	1.860	277	14	2.094	8.80
066	317	0.365	0.902	284	8	1.184	25.40
067	317	0.365	0.902	284	9	1.274	25.30
068	317	0.365	0.902	284	10	1.252	24.60
069	317	0.365	0.902	284	13	1.222	23.47
070	317	0.365	0.902	284	16	1.177	18.97
071	317	0.365	0.902	284	19	1.156	16.13
072	317	0.365	0.902	220	9	1.289	25.50
073	317	0.365	0.902	220	10	1.291	23.10
074	317	0.365	0.902	220	13	1.228	18.73
075	317	0.365	0.902	220	16	1.192	15.70
076	317	0.365	0.902	220	19	1.186	12.47
077	317	0.365	1.186	218	10	1.419	20.63

No.	Po(MPa)	Do(mm)	Dt(mm)	Ma(g/min)	U(cm/min)	Wt(mm)	H(mm)
078	317	0.365	1.186	218	13	1.433	16.07
079	317	0.365	1.186	218	8	1.518	23.37
080	317	0.365	1.186	218	15	1.422	13.97
081	317	0.365	1.186	280	10	1.549	23.57
082	317	0.365	1.186	280	13	1.472	19.02
083	317	0.365	1.186	280	16	1.471	15.53
084	317	0.365	1.186	280	19	1.443	13.03
085	317	0.365	1.790	273	10	2.200	15.60
086	317	0.365	1.790	273	8	2.205	18.70
087	317	0.365	1.790	273	13	2.130	11.80
088	317	0.365	1.790	273	15	2.113	9.17
089	317	0.254	1.155	242	12	1.478	17.47
090	286	0.254	1.155	242	12	1.481	14.52
091	262	0.254	1.155	242	12	1.425	13.14
092	221	0.254	1.155	242	12	1.436	10.52
093	193	0.254	1.179	242	12	1.434	9.02
094	159	0.254	1.179	242	12	1.408	6.83
095	124	0.254	1.179	242	12	1.399	4.09
096	97	0.254	1.179	242	12	1.375	2.54
097	97	0.254	0.916	303	12	1.132	2.65
098	130	0.254	0.916	303	12	1.175	5.06
099	194	0.254	0.916	303	12	1.208	10.84
100	255	0.254	0.916	303	12	1.257	16.13
101	293	0.254	0.958	303	12	1.261	19.01
102	317	0.254	0.958	303	12	1.272	20.89
103	317	0.254	0.958	303	15	1.279	16.73
104	317	0.254	0.958	303	18	1.276	14.44
105	355	0.177	0.894	207	10	1.111	15.54
106	355	0.177	0.894	207	8	1.262	18.51
107	369	0.177	0.894	207	8	1.217	13.34
108	369	0.177	0.894	207	10	1.250	11.21
109	206	0.177	0.894	207	10	1.244	7.77
110	206	0.177	0.894	207	8	1.267	9.11
111	172	0.177	0.894	215	8	1.271	6.78
112	172	0.177	0.894	215	10	1.231	5.47
113	124	0.177	0.894	215	10	1.222	3.01
114	124	0.177	0.894	215	8	1.232	3.79
115	90	0.177	0.894	215	8	1.242	1.81
116	90	0.177	0.894	215	10	1.185	1.30
117	317	0.254	0.865	28	14	1.027	3.10

No.	Po(MPa)	Do(mm)	Dt(mm)	Ma(g/min)	U(cm/min)	Wt(mm)	H(mm)
118	317	0.254	0.865	83	14	1.095	8.16
119	317	0.254	0.865	122	14	1.145	10.93
120	317	0.254	0.865	171	14	1.171	13.64
121	317	0.254	0.865	217	14	1.233	15.48
122	317	0.254	0.865	254	14	1.278	16.77
123	317	0.254	0.865	308	14	1.331	17.41
124	317	0.254	0.865	335	14	1.362	17.55
125	317	0.254	0.865	351	14	1.373	17.53
126	317	0.254	0.865	368	14	1.385	17.18
127	331	0.177	0.906	29	14	1.160	2.22
128	331	0.177	0.906	51	14	1.155	3.87
129	331	0.177	0.906	79	14	1.199	5.87
130	331	0.177	0.906	121	14	1.278	8.15
131	331	0.177	0.906	167	14	1.343	9.30
132	331	0.177	0.906	212	14	1.398	10.33
133	331	0.177	0.906	255	14	1.430	10.15
134	331	0.177	0.906	280	14	1.472	10.30
135	331	0.177	0.906	302	14	1.521	10.45
136	331	0.177	0.906	323	14	1.510	10.06
137	331	0.177	0.906	343	14	1.502	9.84
138	331	0.177	0.906	355	14	1.562	9.80
139	197	0.177	1.015	28	10	1.241	0.82
140	197	0.177	1.015	50	10	1.322	1.58
141	197	0.177	1.015	82	10	1.347	2.62
142	197	0.177	1.015	126	10	1.445	3.77
143	197	0.177	1.015	169	10	1.484	4.50
144	197	0.177	1.015	213	10	1.504	4.99
145	197	0.177	1.015	243	10	1.518	5.20
146	197	0.177	1.015	274	10	1.533	5.35
147	197	0.177	1.015	297	10	1.521	5.40
148	197	0.177	1.015	321	10	1.521	5.36
149	197	0.177	1.015	342	10	1.578	5.49
150	197	0.177	1.015	356	10	1.580	5.52

Database 2

(Use Water Nozzles and Nozzle Body of New Design)
Steel AISI 1018, S_a=50 mesh (Barton's HPE), S_d=2.5 mm

No.	Po(MPa)	Do(mm)	Dt(mm)	Ma(g/min)	U (cm/min)	H(mm)
01	305	0.254	0.830	193	7.62	22.27
02	305	0.254	0.830	193	15.24	12.12
03	305	0.254	0.830	193	10.16	16.58
04	305	0.254	0.830	193	20.32	8.84
05	305	0.254	0.830	265	7.62	23.45
06	305	0.254	0.830	265	10.16	19.72
07	305	0.254	0.830	265	15.24	14.11
08	305	0.254	0.830	265	20.32	10.84
09	317	0.305	1.117	154	7	19.63
10	317	0.305	1.117	154	9	15.47
11	317	0.305	1.117	154	11	12.43
12	317	0.305	1.117	154	14	9.94
13	317	0.305	1.117	197	7	22.53
14	317	0.305	1.117	197	11	16.53
15	317	0.305	1.117	197	12	13.90
16	317	0.305	1.117	197	14	11.81
17	317	0.254	1.089	175	7	19.35
18	317	0.254	1.089	175	9	16.33
19	317	0.254	1.089	175	12	11.40
20	317	0.254	1.089	175	14	10.04
21	317	0.254	1.140	228	7	22.97
22	317	0.254	1.140	228	8	20.29
23	317	0.254	1.140	228	10	16.80
24	317	0.254	1.140	228	12	14.03
25	317	0.254	1.140	228	14	11.62
26	317	0.254	0.869	228	8	22.39
27	317	0.254	0.869	228	9	20.17
28	317	0.254	0.869	228	11	17.00
29	317	0.254	0.869	228	13	14.79
30	317	0.254	0.900	228	15	13.13
31	317	0.254	0.900	180	8	20.36
32	317	0.254	0.900	180	10	16.54
33	317	0.254	0.900	180	12	14.10
34	317	0.254	0.900	180	16	10.84
35	317	0.254	1.773	209	8	12.44
36	317	0.254	1.773	209	6	17.09

37	317	0.254	1.773	209	10	8.67
38	317	0.254	1.773	209	12	7.01

Database 3

(Use Water Nozzles and Nozzle Body of New Design)
Steel AISI 1018, S_a=220 mesh (Barton's HPE), S_d=2.5 mm

No.	Po(MPa)	Do(mm)	Dt(mm)	Ma(g/min)	U(cm/min)	H(mm)
01	317	0.254	0.84	132	6	22.48
02	317	0.254	0.84	132	8	18.41
03	317	0.254	0.84	132	10	14.83
04	317	0.254	0.84	132	12	13.32
05	317	0.254	0.84	155	7	21.25
06	317	0.254	0.84	155	9	17.94
07	317	0.254	0.84	155	12	14.48
08	317	0.254	0.84	155	15	11.86
09	317	0.254	0.84	195	8	21.45
10	317	0.254	0.84	195	11	15.96
11	317	0.254	0.84	195	13	14.45
12	317	0.254	0.84	195	15	12.31
13	317	0.362	1.078	165	7	18.50
14	317	0.362	1.078	165	9	15.17
15	317	0.362	1.078	165	11	12.83
16	317	0.362	1.078	165	13	11.00
17	317	0.362	1.078	202	7	21.35
18	317	0.362	1.078	202	9	17.61
19	317	0.362	1.078	202	11	14.38
20	317	0.362	1.078	202	13	13.13
21	317	0.362	1.078	236	7	23.49
22	317	0.362	1.078	236	9	19.91
23	317	0.362	1.078	236	11	16.10
24	317	0.362	1.078	236	13	14.23

Database 4

(Use Water Nozzles and Nozzle Body of New Nesign)
Titanium, S_a=80 mesh (Barton's HPE), S_d=2.5 mm

No.	Po(MPa)	Do(mm)	Dt(mm)	Ma(g/min)	U(cm/min)	Wt(mm)	H(mm)
01	317	0.254	0.960	27.3	14	1.142	4.33
02	317	0.254	0.960	81.6	14	1.202	11.03
03	317	0.254	0.960	119.5	14	1.254	14.12
04	317	0.254	0.960	162	14	1.320	17.00
05	317	0.254	0.960	162	17	1.310	14.38
06	317	0.254	0.960	162	20	1.308	12.08
07	317	0.254	0.960	162	23	1.307	10.73
08	90	0.178	0.884	214	8	1.112	2.57
09	117	0.178	0.884	214	8	1.110	5.68
10	175	0.178	0.884	214	8	1.165	10.87
11	220	0.178	0.884	214	8	1.274	10.80
12	268	0.178	0.884	214	8	1.259	18.20
13	90	0.178	0.884	214	10	1.075	2.05
14	117	0.178	0.884	214	10	1.106	4.61
15	175	0.178	0.884	214	10	1.179	8.87
16	220	0.178	0.884	214	10	1.200	11.98
17	268	0.178	0.884	214	10	1.266	15.45
18	317	0.254	0.901	235	20	1.266	15.25
19	267	0.254	0.901	235	13	1.291	16.57
20	267	0.254	0.901	235	17	1.290	13.03
21	162	0.254	0.901	235	17	1.254	8.09
22	162	0.254	0.901	235	13	1.293	10.37
23	102	0.254	0.901	235	13	1.212	4.86
24	102	0.254	0.901	235	17	1.207	3.59
25	102	0.254	0.901	235	20	1.176	2.93
26	102	0.254	0.901	235	10	1.274	6.23

Database 5

(Use Water Nozzles and Nozzle Body of New Design)
Aluminum, S_a=80 mesh (Barton's HPE), S_d=2.5 mm

No.	Po(MPa)	Do(mm)	Dt(mm)	Ma(g/min)	U(cm/min)	Wt(mm)	H(mm)
01	317	0.254	0.947	190	25	1.299	21.03
02	317	0.254	0.947	190	28	1.272	19.09
03	317	0.254	0.947	222	28	1.336	19.25
04	317	0.254	0.947	243	28	1.355	20.45
05	317	0.254	0.947	46.6	28	1.243	5.88
06	317	0.254	0.947	95.7	32	1.172	11.02
07	317	0.254	0.947	152	32	1.269	4.49
08	317	0.254	0.947	190	32	1.257	16.69
09	317	0.254	0.947	222	32	1.337	17.36
10	317	0.254	0.947	243	32	1.347	17.92
11	317	0.254	0.947	274	32	1.385	18.68
12	317	0.254	0.947	300	32	1.388	19.52
13	317	0.254	0.947	220	32	1.378	18.74
14	248	0.254	0.947	220	32	1.377	12.28
15	188	0.254	0.947	220	32	1.377	8.30
16	150	0.254	0.947	220	32	1.392	5.74
17	110	0.254	0.947	220	32	1.299	3.05
18	82	0.254	0.947	220	32	1.310	1.53

Database 6

All Predicted Depths of Cut and Percentages of Water Action and Abrasive Action obtained by the Regression Analysis
(Steel AISI 1810, 80 mesh)

No.	C_1H_W	C_2H_a	C_3H_I	$\hat{H}$(mm)	H(mm)	Pw (%)	Pa (%)
001	1.24	22.67	-0.68	19.33	16.83	5.2	94.8
002	0.93	17.00	-0.38	14.43	13.50	5.2	94.8
003	0.74	13.60	-0.24	11.35	10.55	5.2	94.8
004	0.62	11.34	-0.17	9.23	8.77	5.2	94.8
005	0.86	17.16	-0.36	14.62	12.94	4.8	95.2
006	0.69	13.73	-0.23	11.48	10.59	4.8	95.2
007	0.57	11.44	-0.16	9.33	8.78	4.8	95.2
008	1.38	24.60	-1.00	20.53	20.94	6.4	93.6
009	1.30	19.13	-0.60	16.13	17.10	6.4	93.6
010	0.98	14.35	-0.34	11.98	13.43	6.4	93.6
011	0.84	12.30	-0.25	10.12	11.55	6.4	93.6
012	1.58	28.17	-1.00	21.99	23.70	5.7	94.3
013	1.23	20.36	-0.81	17.27	19.05	5.7	94.3
014	0.92	15.27	-0.34	12.84	14.21	5.7	94.3
015	0.79	13.09	-0.25	10.86	12.39	5.7	94.3
016	3.17	33.87	-2.60	25.45	25.60	5.6	94.4
017	2.82	30.11	-2.05	23.32	25.22	5.6	94.4
018	2.54	27.09	-1.66	21.16	23.82	5.6	94.4
019	1.95	20.84	-0.98	17.10	19.16	5.6	94.4
020	1.69	18.06	-0.74	14.95	16.17	5.6	94.4
021	1.49	15.94	-0.56	13.23	14.68	5.6	94.4
022	2.25	27.03	-1.47	21.81	22.83	7.7	92.3
023	1.76	21.24	-0.91	17.59	18.97	7.7	92.3
024	1.45	17.49	-0.61	14.60	15.85	7.7	92.3
025	1.24	14.87	-0.44	12.38	13.55	7.7	92.3
026	1.59	16.84	-0.65	13.96	16.80	8.6	91.4
027	1.36	14.43	-0.47	11.95	14.31	8.6	91.4
028	1.19	12.63	-0.36	10.39	12.65	8.6	91.4
029	1.15	14.07	-0.39	11.69	13.79	7.6	92.4
030	1.32	16.08	-0.51	13.42	15.60	7.6	92.4
031	1.03	12.51	-0.31	10.29	12.16	7.6	92.4
032	1.08	13.18	-0.34	10.90	12.00	7.6	92.4
033	1.30	15.82	-0.50	13.20	14.51	7.6	92.4
034	1.62	19.77	-0.77	16.46	17.80	7.6	92.4
035	0.93	11.30	-0.25	9.20	9.27	7.6	92.4
036	1.59	20.77	-0.80	17.34	18.80	7.1	92.9
037	1.27	16.62	-0.51	13.92	14.58	7.1	92.9
038	1.06	13.85	-0.35	11.51	11.41	7.1	92.9
039	0.91	11.87	-0.26	9.72	8.97	7.1	92.9

No.	C_1Hw	C_2Ha	C_3H_I	$\hat{H}$(mm)	H(mm)	Pw (%)	Pa (%)
040	5.72	46.56	-6.43	26.67	25.50	10.9	89.1
041	5.00	40.74	-4.92	25.64	25.40	10.9	89.1
042	3.64	29.63	-2.60	21.64	20.67	10.9	89.1
043	2.89	23.28	-1.61	18.16	16.57	10.9	89.1
044	2.35	19.17	-1.09	15.44	14.37	10.9	89.1
045	4.33	42.28	-4.42	28.35	25.60	10.9	89.1
046	3.90	38.06	-3.58	26.76	24.80	9.3	90.7
047	3.00	29.27	-2.12	22.42	20.87	9.3	90.7
048	2.44	23.79	-1.40	19.00	16.47	9.3	90.7
049	1.95	19.03	-0.90	15.60	14.30	9.3	90.7
050	2.94	28.95	-2.06	22.27	23.67	9.2	90.8
051	2.26	22.27	-1.22	17.98	19.50	9.2	90.8
052	1.84	18.10	-0.80	14.89	15.50	9.2	90.8
053	1.55	15.24	-0.57	12.60	12.93	9.2	90.8
054	3.03	24.50	-1.79	18.87	18.97	11.0	89
055	2.52	20.42	-1.24	16.29	17.03	11.0	89
056	2.02	16.33	-0.80	13.34	12.70	11.0	89
057	1.68	13.61	-0.55	11.17	10.70	11.0	89
058	2.23	18.04	-0.97	14.61	14.03	11.0	89
059	2.87	23.19	-1.61	18.08	18.23	11.0	89
060	1.82	14.76	-0.65	12.10	9.87	11.0	89
061	1.54	12.49	-0.47	10.22	7.73	11.0	89
062	2.17	21.27	-1.11	17.27	17.00	9.2	90.8
063	1.77	17.41	-0.75	14.35	12.47	9.2	90.8
064	2.79	27.35	-1.84	21.30	20.80	9.2	90.8
065	1.39	13.68	-0.46	11.28	8.80	9.2	90.8
066	6.55	51.05	-8.07	25.99	25.40	11.4	88.6
067	5.82	45.37	-6.37	25.78	25.30	11.4	88.6
068	5.24	40.84	-5.16	25.09	24.60	11.4	88.6
069	4.03	31.41	-3.06	22.17	23.47	11.4	88.6
070	3.27	25.52	-2.01	19.32	18.97	11.4	88.6
071	2.76	21.49	-1.43	16.91	16.13	11.4	88.6
072	5.93	38.15	-5.47	22.00	25.50	13.5	86.5
073	5.34	34.34	-4.43	21.38	23.10	13.5	86.5
074	4.11	26.41	-2.62	18.84	18.73	13.5	86.5
075	3.34	21.46	-1.73	16.37	15.70	13.5	86.5
076	2.81	18.07	-1.23	14.29	12.47	13.5	86.5
077	4.23	27.03	-2.76	19.06	20.63	13.5	86.5
078	3.26	20.80	-1.64	15.97	16.07	13.5	86.5
079	5.29	33.79	-4.32	21.19	23.37	13.5	86.5
080	2.82	18.02	-1.23	14.24	13.97	13.5	86.5
081	4.16	32.06	-3.22	22.35	23.57	11.5	88.5
082	3.20	24.66	-1.90	18.80	19.02	11.5	88.5
083	2.60	20.04	-1.26	15.94	15.53	11.5	88.5
084	2.19	16.88	-0.89	13.70	13.03	11.5	88.5
085	2.93	22.23	-1.58	17.30	15.60	11.7	88.3
086	3.67	27.78	-2.46	20.35	18.70	11.7	88.3
087	2.26	17.10	-0.93	13.84	11.80	11.7	88.3

No.	C_1H_W	C_2H_a	C_3H_I	$\hat{H}$(mm)	H(mm)	Pw (%)	Pa (%)
088	1.96	14.82	-0.70	12.11	9.17	11.7	88.3
089	1.60	18.63	-0.72	15.49	17.47	7.9	92.1
090	1.36	16.36	-0.54	13.65	14.52	7.7	92.2
091	1.19	14.63	-0.42	12.18	13.14	7.5	92.5
092	0.91	11.76	-0.26	9.62	10.52	7.1	92.9
093	0.72	9.69	-0.17	7.68	9.02	6.9	93.1
094	0.53	7.50	-0.10	5.67	6.83	6.5	93.5
095	0.35	5.37	-0.05	3.45	4.09	6.2	93.8
096	0.24	3.84	-0.02	1.89	2.54	5.8	94.2
097	0.28	4.94	-0.03	2.99	2.65	5.3	94.7
098	0.45	7.49	-0.08	5.53	5.06	5.6	94.4
099	0.86	13.00	-0.27	10.77	10.84	6.2	93.8
100	1.33	18.76	-0.60	15.78	16.13	6.6	93.4
101	1.60	21.68	-0.84	18.12	19.01	6.9	93.1
102	1.81	24.04	-1.05	19.90	20.89	7.0	93.0
103	1.45	19.22	-0.67	16.11	16.73	7.0	93.0
104	1.21	16.02	-0.47	13.42	14.44	7.0	93.0
105	1.13	17.94	-0.49	15.18	15.54	5.9	94.1
106	1.42	22.43	-0.77	18.94	18.51	5.9	94.1
107	0.99	16.54	-0.40	13.98	13.34	5.6	94.4
108	0.79	13.23	-0.25	10.99	11.21	5.6	94.4
109	0.51	9.07	-0.11	7.06	7.77	5.3	94.7
110	0.64	11.33	-0.18	9.23	9.11	5.3	94.7
111	0.47	8.76	-0.10	6.76	6.78	5.1	94.9
112	0.37	7.01	-0.06	5.05	5.47	5.1	94.9
113	0.22	4.31	-0.02	2.34	3.01	4.8	95.2
114	0.27	5.39	-0.04	3.42	3.79	4.8	95.2
115	0.16	3.31	-0.01	1.31	1.18	4.5	95.5
116	0.13	2.64	-0.01	0.63	1.30	4.5	95.5
117	2.02	4.25	-0.21	3.40	3.10	32.2	67.8
118	1.94	10.45	-0.49	8.50	8.16	15.7	84.3
119	1.89	13.76	-0.63	11.25	10.93	12.1	87.9
120	1.83	17.01	-0.75	13.98	13.64	9.7	90.3
121	1.78	19.36	-0.83	15.99	15.46	8.4	91.6
122	1.74	20.87	-0.88	17.30	16.77	7.7	92.3
123	1.69	22.61	-0.92	18.82	17.41	6.9	93.1
124	1.66	23.30	-0.93	19.75	17.55	6.7	93.3
125	1.65	23.66	-0.94	19.77	17.53	6.5	93.5
126	1.63	24.02	-0.94	20.09	17.18	6.4	93.6
127	0.98	4.04	-0.10	2.57	2.22	19.6	80.4
128	0.95	6.20	-0.14	4.53	3.87	13.3	86.7
129	0.92	8.25	-0.18	6.39	5.87	10.0	90.0
130	0.87	10.33	-0.22	8.30	8.15	7.8	92.2
131	0.82	11.72	-0.23	9.59	9.30	6.6	93.4
132	0.78	12.53	-0.24	10.35	10.33	5.8	94.2
133	0.74	12.98	-0.23	10.76	10.15	5.4	94.6
134	0.72	13.13	-0.23	10.91	10.30	5.2	94.8
135	0.70	13.21	-0.23	10.99	10.45	5.1	94.9
136	0.69	13.26	-0.22	11.04	10.06	4.9	95.1
137	0.67	13.28	-0.22	11.06	9.84	4.8	95.2

No.	C_1Hw	C_2Ha	C_3H_I	$\hat{H}$(mm)	H(mm)	Pw (%)	Pa (%)
138	0.67	13.28	-0.21	11.06	9.80	4.8	95.2
139	0.57	2.84	-0.04	1.15	0.82	16.7	83.3
140	0.55	4.28	-0.06	2.52	1.58	11.3	88.7
141	0.52	5.69	-0.07	3.84	2.62	8.3	91.7
142	0.48	6.81	-0.08	4.90	3.77	6.6	93.4
143	0.45	7.38	-0.08	5.43	4.59	5.7	94.3
144	0.42	7.66	-0.08	5.69	4.99	5.2	94.8
145	0.40	7.73	0.08	5.76	5.20	5.0	95.0
146	0.39	7.75	-0.07	5.77	5.35	4.8	95.2
147	0.38	7.73	-0.07	5.74	5.40	4.6	95.4
148	0.36	7.69	-0.07	5.70	5.36	4.5	95.5
149	0.35	7.64	-0.07	5.65	5.49	4.4	95.6
150	0.35	7.61	-0.06	5.61	5.52	4.3	95.7

Database 7

The Predicted Velocity Distribution
(Steel AISI 1810, Size of Abrasive = 80 mesh)

No.	Ma/Mw	Vsw	Vcw	Va	Vcw/Vsw	Va/Vsw	Va/Vcw	H(mm)
001	0.235	796	645	400	0.81	0.502	0.62	16.83
002	0.235	796	645	400	0.81	0.502	0.62	13.50
003	0.235	796	645	400	0.81	0.502	0.62	10.55
004	0.235	796	645	400	0.81	0.502	0.62	8.77
005	0.294	796	615	355	0.773	0.446	0.578	12.94
006	0.294	796	615	355	0.773	0.446	0.578	10.59
007	0.249	796	615	355	0.773	0.446	0.578	8.78
008	0.148	796	694	490	0.871	0.616	0.707	20.94
009	0.148	796	694	490	0.871	0.616	0.707	17.10
010	0.148	796	694	490	0.871	0.616	0.707	13.43
011	0.148	796	694	490	0.871	0.616	0.707	11.55
012	0.189	796	670	443	0.841	0.557	0.662	23.70
013	0.189	796	670	443	0.841	0.557	0.662	19.05
014	0.189	796	670	443	0.841	0.557	0.662	14.21
015	0.189	796	670	443	0.841	0.557	0.662	12.39
016	0.087	796	732	582	0.92	0.731	0.795	25.60
017	0.087	796	732	582	0.92	0.731	0.795	25.22
018	0.087	796	732	582	0.92	0.731	0.795	23.82
019	0.087	796	732	582	0.92	0.731	0.795	19.16
020	0.087	796	732	582	0.92	0.731	0.795	16.17
021	0.087	796	732	582	0.92	0.731	0.795	14.68
022	0.106	796	720	551	0.904	0.692	0.765	22.83
023	0.106	796	720	551	0.904	0.692	0.765	18.97
024	0.106	796	720	551	0.904	0.692	0.765	15.85
025	0.106	796	720	551	0.904	0.692	0.765	13.55
026	0.086	796	733	584	0.921	0.733	0.796	16.80
027	0.086	796	733	584	0.921	0.733	0.796	14.31
028	0.086	796	733	584	0.921	0.733	0.796	12.65
029	0.108	796	718	547	0.902	0.687	0.761	13.79
030	0.108	796	718	547	0.902	0.687	0.761	15.60
031	0.108	796	718	547	0.902	0.687	0.761	12.16
032	0.108	796	718	547	0.902	0.687	0.761	12.00
033	0.108	796	718	547	0.902	0.687	0.761	14.51
034	0.108	796	718	547	0.902	0.687	0.761	17.80
035	0.108	796	718	547	0.902	0.687	0.761	9.27
036	0.122	796	710	526	0.891	0.661	0.741	18.80
037	0.122	796	710	526	0.891	0.661	0.741	14.58
038	0.122	796	710	526	0.891	0.661	0.741	11.41
039	0.060	796	710	526	0.891	0.661	0.741	8.97
040	0.060	796	751	636	0.944	0.799	0.847	25.50
041	0.060	796	751	636	0.944	0.799	0.847	25.40
042	0.060	796	751	636	0.944	0.799	0.847	20.67

No.	Ma/Mw	Vsw	Vcw	Va	Vcw/Vsw	Va/Vsw	Va/Vcw	H(mm)
043	0.060	796	751	636	0.944	0.799	0.847	16.57
044	0.060	796	751	636	0.944	0.799	0.847	14.37
045	0.077	796	739	601	0.928	0.754	0.813	25.60
046	0.077	796	739	601	0.928	0.754	0.813	24.80
047	0.077	796	739	601	0.928	0.754	0.813	20.87
048	0.077	796	739	601	0.928	0.754	0.813	16.47
049	0.077	796	739	601	0.928	0.754	0.813	14.30
050	0.078	796	739	599	0.928	0.752	0.811	23.67
051	0.078	796	739	599	0.928	0.752	0.811	19.50
052	0.078	796	739	599	0.928	0.752	0.811	15.50
053	0.078	796	739	599	0.928	0.752	0.811	12.93
054	0.059	796	752	638	0.944	0.801	0.848	18.97
055	0.059	796	752	638	0.944	0.801	0.848	17.03
056	0.059	796	752	638	0.944	0.801	0.848	12.70
057	0.059	796	752	638	0.944	0.801	0.848	10.70
058	0.059	796	752	638	0.944	0.801	0.848	14.03
059	0.059	796	752	638	0.944	0.801	0.848	18.23
060	0.059	796	752	638	0.944	0.801	0.848	9.87
061	0.059	796	752	638	0.944	0.801	0.848	7.73
062	0.078	796	739	600	0.928	0.753	0.812	17.00
063	0.078	796	739	600	0.928	0.753	0.812	12.47
064	0.078	796	739	600	0.928	0.753	0.812	20.80
065	0.078	796	739	600	0.928	0.753	0.812	8.80
066	0.057	796	735	642	0.946	0.807	0.853	25.40
067	0.057	796	735	642	0.946	0.807	0.853	25.30
068	0.057	796	735	642	0.946	0.807	0.853	24.60
069	0.057	796	735	642	0.946	0.807	0.853	23.47
070	0.057	796	735	642	0.946	0.807	0.853	18.97
071	0.057	796	735	642	0.946	0.807	0.853	16.13
072	0.044	796	763	672	0.958	0.844	0.881	25.50
073	0.044	796	763	672	0.958	0.844	0.881	23.10
074	0.044	796	763	672	0.958	0.844	0.881	18.73
075	0.044	796	763	672	0.958	0.844	0.881	15.70
076	0.044	796	763	672	0.958	0.844	0.881	12.47
077	0.044	796	763	673	0.958	0.845	0.882	20.63
078	0.044	796	763	673	0.958	0.845	0.882	16.07
079	0.044	796	763	673	0.958	0.845	0.882	23.37
080	0.044	796	763	673	0.958	0.845	0.882	13.97
081	0.056	796	754	644	0.947	0.809	0.854	23.57
082	0.056	796	754	644	0.947	0.809	0.854	19.02
083	0.056	796	754	644	0.947	0.809	0.854	15.53
084	0.056	796	754	644	0.947	0.809	0.854	13.03
085	0.055	796	755	647	0.948	0.813	0.857	15.60
086	0.055	796	755	647	0.948	0.813	0.857	18.70
087	0.055	796	755	647	0.948	0.813	0.857	11.80
088	0.055	796	755	647	0.948	0.813	0.857	9.17
089	0.100	796	724	560	0.909	0.704	0.774	17.47
090	0.105	756	684	524	0.905	0.693	0.766	14.52
091	0.110	724	652	495	0.901	0.683	0.758	13.14

No.	Ma/Mw	Vsw	Vcw	Va	Vcw/Vsw	Va/Vsw	Va/Vcw	H(mm)
092	0.120	665	594	442	0.893	0.665	0.744	10.52
093	0.128	621	551	403	0.886	0.649	0.733	9.02
094	0.141	564	494	354	0.876	0.627	0.715	6.83
095	0.16	498	429	298	0.862	0.597	0.693	4.09
096	0.181	440	373	250	0.847	0.568	0.670	2.54
097	0.226	440	359	225	0.815	0.512	0.628	2.65
098	0.195	510	427	280	0.836	0.548	0.655	5.06
099	0.160	623	537	372	0.862	0.597	0.693	10.84
100	0.140	714	627	450	0.878	0.630	0.718	16.13
101	0.130	766	677	494	0.885	0.646	0.730	19.01
102	0.125	796	708	521	0.889	0.655	0.737	20.89
103	0.125	796	708	521	0.889	0.655	0.737	16.73
104	0.125	796	708	521	0.889	0.655	0.737	14.44
105	0.171	819	699	475	0.854	0.581	0.680	15.54
106	0.171	818	699	475	0.854	0.581	0.680	18.51
107	0.191	733	616	406	0.840	0.554	0.660	13.34
108	0.191	733	616	406	0.840	0.554	0.660	11.21
109	0.218	642	527	334	0.821	0.521	0.634	7.77
110	0.218	642	527	334	0.821	0.521	0.634	9.11
111	0.246	587	470	287	0.801	0.489	0.610	6.78
112	0.248	587	470	287	0.801	0.489	0.610	5.47
113	0.292	498	385	223	0.744	0.448	0.579	3.01
114	0.292	498	385	223	0.744	0.448	0.579	3.79
115	0.343	424	316	173	0.744	0.409	0.549	1.81
116	0.343	424	316	173	0.744	0.409	0.549	1.30
117	0.012	796	787	759	0.989	0.954	0.965	3.10
118	0.034	796	770	696	0.967	0.874	0.904	8.16
119	0.050	796	758	657	0.952	0.825	0.866	10.93
120	0.071	796	744	614	0.934	0.771	0.825	13.64
121	0.090	796	731	578	0.918	0.726	0.791	15.46
122	0.105	796	721	552	0.905	0.693	0.766	16.77
123	0.127	796	706	518	0.887	0.651	0.734	17.41
124	0.138	796	699	503	0.878	0.632	0.719	17.55
125	0.145	796	695	494	0.873	0.621	0.711	17.53
126	0.152	796	691	485	0.868	0.609	0.702	17.18
127	0.024	814	794	738	0.976	0.908	0.93	2.22
128	0.042	814	780	690	0.959	0.848	0.884	3.87
129	0.066	814	763	637	0.938	0.783	0.834	5.87
130	0.101	814	739	571	0.908	0.702	0.773	8.15
131	0.139	814	714	513	0.878	0.631	0.718	9.30
132	0.176	814	692	467	0.850	0.573	0.675	10.33
133	0.212	814	671	429	0.825	0.528	0.640	10.15
134	0.233	814	660	410	0.811	0.504	0.622	10.30
135	0.251	814	650	395	0.799	0.486	0.608	10.45
136	0.269	814	641	381	0.788	0.469	0.595	10.06
137	0.286	814	633	369	0.778	0.454	0.583	9.84
138	0.296	814	628	362	0.772	0.445	0.577	9.80
139	0.030	628	609	557	0.971	0.887	0.914	0.82
140	0.054	628	596	511	0.949	0.815	0.859	1.58

No.	Ma/Mw	Vsw	Vcw	Va	Vcw/Vsw	Va/Vsw	Va/Vcw	H(mm)
141	0.088	628	577	457	0.919	0.728	0.793	2.62
142	0.136	628	553	399	0.88	0.636	0.722	3.77
143	0.182	628	531	355	0.846	0.565	0.669	4.59
144	0.230	628	510	319	0.813	0.508	0.625	4.99
145	0.262	628	497	298	0.792	0.475	0.600	5.20
146	0.296	628	484	279	0.772	0.445	0.577	5.35
147	0.321	628	475	267	0.757	0.425	0.562	5.40
148	0.346	628	466	255	0.743	0.407	0.547	5.36
149	0.369	628	458	246	0.730	0.391	0.536	5.49
150	0.384	628	453	240	0.722	0.382	0.528	5.52

Database 8

The Predicted Velocity Distribution
(Steel AISI 1810, Size of Abrasive = 50 mesh)

No.	Ma/Mw	Vw	Vcw	Va	Vcw/Vw	Va/Vw	Va/Vcw	H(mm)
01	0.081	781	722	582	0.925	0.745	0.805	22.27
02	0.081	781	722	582	0.925	0.745	0.805	12.12
03	0.081	781	722	582	0.925	0.745	0.805	16.58
04	0.081	781	722	582	0.925	0.745	0.805	8.84
05	0.112	781	722	531	0.900	0.680	0.756	23.45
06	0.112	781	722	531	0.900	0.680	0.756	19.72
07	0.112	781	722	531	0.900	0.680	0.756	14.11
08	0.112	781	722	531	0.900	0.680	0.756	10.84
09	0.044	796	763	671	0.958	0.843	0.880	19.63
10	0.044	796	763	671	0.958	0.843	0.880	15.47
11	0.044	796	763	671	0.958	0.843	0.880	12.43
12	0.044	796	763	671	0.958	0.843	0.880	9.94
13	0.056	796	754	643	0.947	0.808	0.853	22.53
14	0.056	796	754	643	0.947	0.808	0.853	16.53
15	0.056	796	754	643	0.947	0.808	0.853	13.90
16	0.056	796	754	643	0.947	0.808	0.853	11.81
17	0.072	796	742	610	0.933	0.766	0.822	19.35
18	0.072	796	742	610	0.933	0.766	0.822	16.33
19	0.072	796	742	610	0.933	0.766	0.822	11.40
20	0.072	796	742	610	0.933	0.766	0.822	10.04
21	0.094	796	728	570	0.914	0.716	0.783	22.97
22	0.094	796	728	570	0.914	0.716	0.783	20.29
23	0.094	796	728	570	0.914	0.716	0.783	16.80
24	0.094	796	728	570	0.914	0.716	0.783	14.03
25	0.094	796	728	570	0.914	0.716	0.783	11.62
26	0.094	796	728	570	0.914	0.716	0.783	22.39
27	0.094	796	728	570	0.914	0.716	0.783	20.17
28	0.094	796	728	570	0.914	0.716	0.783	17.00
29	0.094	796	728	570	0.914	0.716	0.783	14.79
30	0.094	796	728	570	0.914	0.716	0.783	13.13
31	0.094	796	741	606	0.931	0.761	0.818	20.36
32	0.074	796	741	606	0.931	0.761	0.818	16.54
33	0.074	796	741	606	0.931	0.761	0.818	14.10
34	0.074	796	741	606	0.931	0.761	0.818	10.84
35	0.086	796	733	584	0.921	0.733	0.796	12.44
36	0.086	796	733	584	0.921	0.733	0.796	17.09
37	0.086	796	733	584	0.921	0.733	0.796	8.67
38	0.086	796	733	584	0.921	0.733	0.796	7.01

Database 9

The Predicted Velocity Distribution
(Steel AISI 1810,Size of Abrasive = 220 mesh)

No.	Ma/Mw	Vw	Vcw	Va	Vcw/Vw	Va/Vw	Va/Vcw	H(mm)
01	0.055	796	755	647	0.948	0.813	0.857	22.48
02	0.055	796	755	647	0.948	0.813	0.857	18.41
03	0.055	796	755	647	0.948	0.813	0.587	14.83
04	0.055	796	755	647	0.948	0.813	0.587	13.32
05	0.064	796	748	627	0.940	0.787	0.838	21.25
06	0.064	796	748	627	0.940	0.787	0.838	17.94
07	0.064	796	748	627	0.940	0.787	0.838	14.48
08	0.064	796	748	627	0.940	0.787	0.838	11.86
09	0.081	796	737	594	0.925	0.747	0.807	21.45
10	0.081	796	737	594	0.925	0.747	0.807	15.96
11	0.081	796	737	594	0.925	0.747	0.807	14.45
12	0.081	796	737	594	0.925	0.747	0.807	12.31
13	0.034	796	770	698	0.968	0.876	0.905	18.50
14	0.034	796	770	698	0.968	0.876	0.905	15.17
15	0.034	796	770	698	0.968	0.876	0.905	12.89
16	0.034	796	770	698	0.968	0.876	0.905	11.00
17	0.041	796	765	679	0.961	0.852	0.887	21.35
18	0.041	796	765	679	0.961	0.852	0.887	17.61
19	0.041	796	765	679	0.961	0.852	0.887	14.38
20	0.041	796	765	679	0.961	0.852	0.887	13.13
21	0.048	796	760	662	0.954	0.832	0.872	23.49
22	0.048	796	760	662	0.954	0.832	0.872	19.91
23	0.048	796	760	662	0.954	0.832	0.872	16.19
24	0.048	796	760	662	0.954	0.832	0.872	14.23

WORKS CITED

1. Ohya, H. and M. Hoshina. "Research and Development into Ultra-high Pressure Jet Boring Machine" *Proceedings of the 10th International Symposium on Jet Cutting Technology*. Amsterdam (1990).

2. Geskin, E.S., W.L. Chen and W.Z. Lee. "Glass Shaping by the Use of Abrasive Waterjet." *Glass Digest*. November, 1989, pp. 60-64.

3. Vora, A. "Investigation of the Characteristics of the Kerf and the Surface Generated in the Course of Cutting Titanium with Abrasive Waterjet" *Master's Thesis*. New Jersey Institute of Technology, May 1988.

4. Hashish, M. "Application of Abrasive Waterjet to Metal Cutting". *Proceedings of Conference on Nontraditional Machining*. 1986, pp. 1-11.

5. Hashish, M., "Turning, Milling and Drilling with Abrasive-Waterjet (AWJ)". *Proceedings of the 9th International Symposium on Jet Cutting Technology*. October, 1988, pp. 113-132.

6. Hu, F., Y. Yang, E,S. Geskin and Y. Chung. "Characterization of Material Removal in the Course of Abrasive Waterjet Machining". *Proceedings of the 6th American Water Jet Conference*. Houston (1990), pp. 17-29.

7. Hu, F. "Investigation of Material Erosion by Abrasive Water Cutting". *Master's Thesis*. New Jersey Institute of Technology, May 1990.

8. Hashish, M. "Prediction Equations Relating High Velocity Jet Cutting Performance to Stand Off Distance and Multipasses". *Journal of Engineering Industry*. August 1979, Vol. 101, pp.311-318.

9. Shih, L.Y. "Development of Technology for Glass Shaping by the Use of Abrasive Water-jet". *Master's Thesis*. New Jersey Institute of Technology. September 1991.

10. I. Finnie, A. Levy, and D.H. Mcfadden, "Fundamental Mechanisms of Erosive Wear of Ductile Metals by Solid Particles". *Erosion: Prevention and Useful Applications*. ASTM Stp 664, 1979, pp.36-58.

11. Bitter, J. G. A., "A Study of Erosion Phenomena - Part I" *Wear*, Vol 6, 1963, pp.5-21.

12. Bitter, J. G. A., "A Study of Erosion Phenomena - Part II" *Wear*, Vol 6, 1963, pp.169-190.

13. G. P. Tilly, "A Two Stage Mechanism of Ductile Erosion", *Wear*, Vol. 23, 1973, pp87-96.

14. J. Maji and G. L. Sheldon, " Mechanisms of Erosion of a Ductile Material by Solid Particles", E*rosion: Prevention and Useful Applications*, ASTM Stp 664, 1979, pp. 136-147.

15. I. M. Hutchings, "Mechanisms of the Erosion of Metal by Solid Particles", *Erosion: Prevention and Useful Applications*, ASTM Stp 664, 1979, pp. 59-76.

16. C. E. Smeltzer, M. E. Gulden, W. A. Compton, "Mechanism of Metal Removal by Impacting Dust Particles", *Journal of Basic Engineering*, Sept, 1970, pp. 639-654.

17. Ambrish Misra, Iain Finnie, "On the Size Effect in Abrasive Waterjet", *Wear*, Vol. 65, 1981, pp. 359-373.

18. Hashish. M, "A Modeling Study of Metal Cutting with Abrasive Waterjet", *Journal of Engineering Material and Technology*, Vol. 106, Jan. 1984, pp. 88-100.

19. Donald D. Davis, *Nontraditional Manufacturing Process*, Jossey-Bass, 1980, pp157-193

20. Finnie, I. "Erosion of Surfaces By Solid Particles". *Wear*. Vol. 3, 1960, pp. 87-103.

21. Bitter, J.G.A. "A Study of Erosion Phenomena - Part I and Part II". *Wear*. Vol. 6, 1963, pp. 169-190.

22. Neilson, J.H. and A. Gilchrist. "Erosion by a Stream of Solid Particles". *Wear*. Vol.II, 1968, pp.111-122.

23. Preece, C., ed., *Erosion*, Vol. 16 Academic Press, New York, 1979, pp.69-126.

24. Engel, P., *Impact Wear of Materials*, Elsevier Scientific Publishing Co., Amsterdam-Oxford, New York, 1976, pp.104-158.

25. T. J. Labus. "A Comparison of Pulsed Jets Versus Mechanical Breakers". *the Sixth International Symposium on Jet Cutting*, 1983. pp. 229- 238.

26. Hashish, M. "A Model for Abrasive-Waterjet (AWJ) Machining". *ASME Journal of Engineering Materials and Technology*. Apr. 1989, Vol. 111, pp.154-162.

27. Y, Chung. "Development of Prediction Technique for the Geometry of the Abrasive Waterjet Generated Kerf". *Master Thesis*. New Jersey Institute of Technology, May, 1992.

28. Finnie, I., "Erosion by Solid Particle in a Fluid Stream", *ASTM Technical Publication* 307, 1961

29. Soo, S. L., *Fluid Dynamics of Multiphase System,* Waltham, Mass., Blaisdell Pub. Co., 1967.

30. Sheldon, G. L. and Finnie, I., "The Mechanism of Material Removal in the Erosive Cutting of Brittle Material", *Journal of Engineering for Industry*, Nov. 1966.

31. Finnie, I., Wolak J. and Kabil, Y. "Erosion of Metals by Solid Particles", *Journal of Materials,* 1967.

33. Tilly, G.P., "Erosion Caused by Airborne Particles", *Wear* 14, 1969.

34. Sheldon, G. L. and Kanhere, A., "An Investigation of Impingement Erosion Using Single Particle", *Wear* 21, 1972.

35. Young, J. P. and Ruff, A. W., "Particle Erosion Measurements on Metals", *Journal of Engineering Materials and Technology,* April, 1977.

36. Benchaita, M. T., Griffith, P. and Rabinowicz, E., "Erosion of Metallic Plate by Solid Particles Entrained in a Liquid Jet", *Journal of Engineering for Industry,* August, 1983.

37. Verma, A.P. and Lal, G.K., "An Experimental Study of Abrasive Machining", *Int. J. Mach. Tools Des. Res.,* Vol. 24, 1984.

38. Verma, A.P. and Lal, G.K., "Basic Mechanics of Abrasive Jet Machining", *IE (I) Journal-PE* , 1985.

39. Michaelides, E.E., "Motion of Particles in Gases: Average Velocity and Pressure Loss", *Transactions of the ASME*, Vol. 109, June, 1987.

40. Hinze, J.O., *Turbulence*, McGraw-Hill Book Company, Inc., 1959.

41. Tchen, C.M., "Mean Values and Correlation Problems Connected with the Motion of Small Particles", *Ph.D. Thesis,* Delft, 1947.

42. Hjelmfelt, A.T., Jr. and Mockros, L.F., "Motion of Discrete Particles in a Turbulent Fluid" *Appl. Sci. Res.*, 1965.

43. Danon, H., Wolfshtein, M. and Hetsroni, G., " Numerical Calculation of Two-Phase Turbulent Round Jet ", *Int. J. Multiphase Flow*, Vol.. 3, 1977, pp. 223-234.

44. Melville, W.K. and bray, K.N.C., " A Model of the Two-Phase Turbulent Jet ", *Int. J. Heat Mass Transfer*, Vol. 22, 1979.

45. Maxey, M.R., and Riley, J.J., " Equation of Motion for a Small Rigid Sphere in a Non uniform Flow ", *Phys. Fluids*, 26(4), April 1983.

46. Situ, M. and Schetz, J.A., "Numerical Calculations of the Breakup of Highly Loaded Slurry Jets", *Journal of Fluids Engineering*, Sep. 1987.

47. Givler, R.C. and Mikatarian, R.R., "Numerical Simulation of Fluid-Particle Flows: Geothermal Drilling Applications", *Journal of Fluids Engineering* , Sep., 1987.

48. Ahmadi, G. and Ounis, H., "Dispersion of Small Rigid Spheres in a Turbulent Flow Field", *Proceedings of International Conference on Mechanics of Two-Phase Flow*, June, 1989.

49. Hashish, M., "On the Modeling of Abrasive-waterjet Cutting", *Proceedings of 7th International Symposium on Jet Cutting Technology*, 1984, pp. 249-265.

50. Isobe, T., Yoshida, H. and Nishi, K., " Distribution of Abrasive Particles in Abrasive Water Jet and Acceleration Mechanism ", Proceedings of 9th International Symposium on Jet Cutting Technology, 1988.

51. Chen, W.L. "Correlation Between Particles Velocities and Conditions of Abrasive Waterjet Formation", Ph.D. Dissertation. New Jersey Institute of Technology, January, 1990.

52. J. Wesley Barnes, *Statistical Analysis for Engineers*, Prentice Hall Inc. 1988.

53. O. J. Dunn, V. A. Clark, *Applied Statistics: Analysis of Variance and Regression*, J.Wiley & Sons, pp. 221-306.

54. K. A. Brownlee, *Statistical Theory and Methodology in Science and Engineering*, Wiley, pp. 334-554.